



**ESC**

European Society  
of Cardiology

European Journal of Heart Failure (2020) **23** (Suppl. S1) n/a  
doi:10.1002/ejhf.2100

## Chronic Heart Failure – Pathophysiology and Mechanisms

### Analysis of the pathophysiology of heart failure with reduced and preserved ejection fraction: a non-invasive hemodynamic evaluation

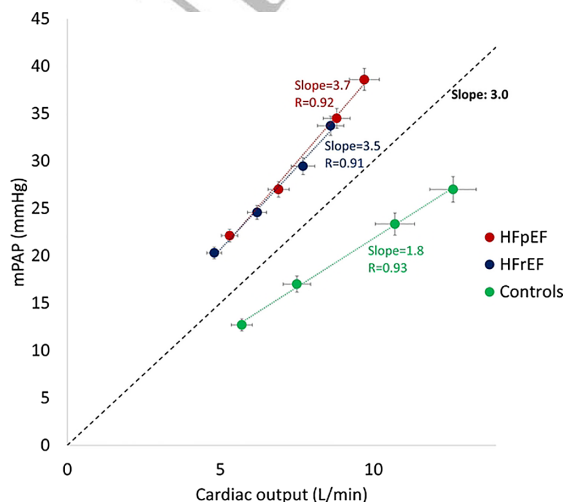
NR Pugliese<sup>1</sup>; M Matteo Mazzola<sup>1</sup>; N De Biase<sup>1</sup>; L Gargani<sup>2</sup>; I Fabiani<sup>3</sup>; FL Dini<sup>4</sup>; E Bossone<sup>5</sup>; P Frumento<sup>1</sup>; S Taddei<sup>1</sup>; BA Borlaug<sup>6</sup>; S Masi<sup>1</sup>; <sup>1</sup>University of Pisa, Pisa, Italy; <sup>2</sup>National Council of Research, Pisa, Italy; <sup>3</sup>Fondazione Toscana Gabriele Monasterio, Pisa, Italy; <sup>4</sup>Casa di Cura Villa Esperia, Area Cardiologica, Salice Terme, Pavia, Italy; <sup>5</sup>Cardarelli Hospital, Naples, Italy; <sup>6</sup>Mayo Clinic, Rochester, USA;

### Funding Acknowledgements: None

**Background:** Prior studies have demonstrated key differences in heart failure patients with reduced (HFrEF) vs preserved ejection fraction (HFpEF), but have been confounded by baseline differences in age, body composition, and functional disability. We used combined cardiopulmonary-exercise stress echocardiography (CPET-ESE) to analyse the differences in the HF phenotypes after matching for these baseline factors.

**Methods:** Subjects with HFrEF (n=70) and HFpEF (n=70) were matched 1:1 for age, sex, body mass index, peak oxygen consumption, and minute ventilation/carbon dioxide production slope. All the patients performed a symptom-limited graded ramp bicycle CPET-ESE.

**Results:** During a median follow-up of 23 months, there were 10 deaths and 67 HF hospitalisations. The distribution of events was not different between HFpEF and HFrEF. Multipoint mean pulmonary artery pressure (mPAP)/cardiac output (CO) slopes were similar in HFrEF and HFpEF ( $3.7 \pm 1.5$  and  $3.5 \pm 1.8$  mmHg/L/min) (Figure 1). Right ventricle-pulmonary artery (RV-PA) coupling was more severely deranged in HFpEF than HFrEF (peak tricuspid annular plane systolic excursion/systolic pulmonary artery pressure  $0.42 \pm 0.2$  vs  $0.55 \pm 0.2$  mm/mmHg in HFrEF;  $P < 0.01$ ), as well as left atrium-left ventricle (LA-LV) interaction (LA reservoir strain/LV global longitudinal strain at low-load effort  $1.5 \pm 0.8$  vs  $2.2 \pm 1.1$  in HFrEF;  $P < 0.01$ ). When compared to HFrEF, subjects with HFpEF displayed a higher prevalence of metabolic syndrome and higher values of high-sensitivity C-reactive protein (3.68, interquartile range [IQR] 2.12–5.66 vs. 2.19, IQR 1.37–4.97 mg/L;  $P < 0.01$ ).



mPAP/CO slope for each group

**Conclusions:** Despite similar baseline characteristics and disease severity, HFpEF and HFrEF reflect different pathophysiological mechanisms. RV-PA/LA-LV uncoupling, low-grade systemic inflammation and metabolic syndrome are more common in patients with HFpEF than HFrEF.

### Plasma P-Selectin: a prognostic biomarker in heart failure with preserved ejection fraction

P Prathap Kanagala<sup>1</sup>; JR Arnold<sup>2</sup>; JN Khan<sup>2</sup>; A Singh<sup>2</sup>; GS Gulsin<sup>2</sup>; S Kotha<sup>1</sup>; IB Squire<sup>2</sup>; Gp Mccann<sup>2</sup>; LL Ng<sup>2</sup>; <sup>1</sup>Liverpool University Hospitals NHS Trust, Liverpool, UK; <sup>2</sup>NIHR Biomedical Research Unit in Cardiovascular Disease, Leicester, UK;

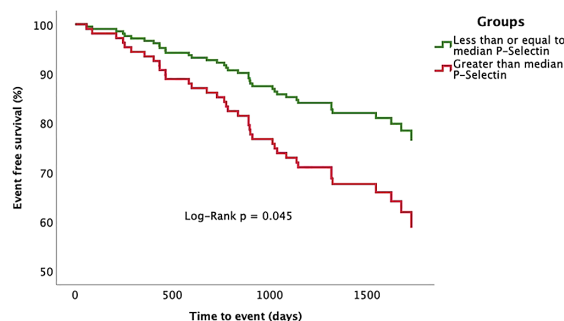
**Funding Acknowledgements:** National Institute for Health Research (NIHR) Leicester Cardiovascular Biomedical Research Centre [overall project Grant IRS\_BRU\_0211\_20033]

**Background:** The Selectins are integral mediators of platelet activation and endothelial function and have been implicated in the pathophysiology of heart failure with preserved ejection fraction (HFpEF).

**Purpose:** To assess the association of P-Selectin with mortality in HFpEF.

**Methods:** Prospective, observational study of 130 HFpEF patients (mean age  $72 \pm 10$ , males 50%) who underwent extensive phenotyping with blood sampling, six-minute walk testing, echocardiography, cardiovascular magnetic resonance imaging (CMR), calculation of the Meta-Analysis Global Group in Chronic Heart Failure Risk (MAGGIC) scores and blinded plasma P-Selectin measurement.

**Results:** Overall, HFpEF was characterised by a high burden of co-morbidity: hypertension 91%; obesity 63%; diabetes 50% and metrics of diastolic dysfunction: B-type natriuretic peptide (BNP)  $140$  [66–258] ng/L; left ventricular mass indexed (LVMI)  $53 \pm 15$  g/m<sup>2</sup>; maximal left atrial volume indexed (LAVImax)  $54 \pm 26$  ml/m<sup>2</sup>; E/E'  $13 \pm 5$ . The HFpEF sub-group with higher P-Selectin levels (median 26372 [19360–34889] pg/ml) was associated with lower age, higher heart rate, less prevalent atrial fibrillation, less frequent current smoking status and lower right ventricular end-diastolic volumes. During follow-up (median 1428 days), there were 38 endpoints (all-cause deaths).



Kaplan-Meier Survival Analysis

Above median P-Selectin levels were associated with greater risk of all-cause mortality (HR 1.974; CI 1.016–3.837; Log-Rank  $P < 0.045$  – see Figure). Excluding components of the MAGGIC score, there were 12 parameters demonstrating univariate association with the endpoint of  $P < 0.1$  including: diastolic blood pressure, previous HF hospitalization, loop diuretic use, haemoglobin, BNP, echocardiographic E/E', LVMI, indexed right ventricular end-diastolic and end-systolic volumes, LAVImax, myocardial infarction (MI) detected by CMR and plasma P-Selectin. Following multivariable Cox proportional hazards regression analysis and when added to MAGGIC scores, only P-Selectin (adjusted hazard ratio [HR] 1.707; 95% confidence interval [CI] 1.099–2.650;  $P < 0.017$ ) and MI detected by CMR (HR 2.377; CI 1.114–5.075;

$P < 0.025$ ) remained significant predictors. In a final model comprising all 3 parameters, only P-Selectin (HR 1.447; CI 1.130–1.853;  $P < 0.003$ ) and MAGGIC scores (HR 1.555; CI 1.136–2.129;  $P < 0.006$ ) remained independent predictors of death. Adding P-Selectin (0.618,  $P = 0.035$ ) improved the area under the curve for mortality prediction for MAGGIC scores (0.647,  $P = 0.009$ ) to 0.710,  $P < 0.0001$ .

**Conclusions:** Plasma P-Selectin is an independent predictor of mortality and adds prognostic value to MAGGIC scores in HFpEF.

### Nicotinamide treats cardiac hallmarks of experimental heart failure with preserved ejection fraction

M Abdellatif<sup>1</sup>; V Trummer-Herbst<sup>1</sup>; F Koser<sup>2</sup>; D Sylvere<sup>3</sup>; R Adao<sup>4</sup>; F Vasques-Nova<sup>4</sup>; JK Freundt<sup>2</sup>; D Von Lewinski<sup>1</sup>; AF Leite-Moreira<sup>4</sup>; Ap Lourenco<sup>4</sup>; J Alegre-Cebollada<sup>5</sup>; S Kiechl<sup>6</sup>; WA Linke<sup>2</sup>; G Kroemer<sup>3</sup>; S Sedej<sup>1</sup>; <sup>1</sup>Medical University of Graz, Department of Cardiology, Graz, Austria; <sup>2</sup>University of Muenster, Institute of Physiology II, Muenster, Germany; <sup>3</sup>Gustave Roussy Cancer Institute, Metabolomics and Cell Biology Platforms, Villejuif, France; <sup>4</sup>Faculty of Medicine University of Porto, Department of Surgery and Physiology, Cardiovascular Research and Development Centre (UnIC), Porto, Portugal; <sup>5</sup>National Centre for Cardiovascular Research (CNIC), Madrid, Spain; <sup>6</sup>Medical University of Innsbruck, Department of Neurology, Innsbruck, Austria;

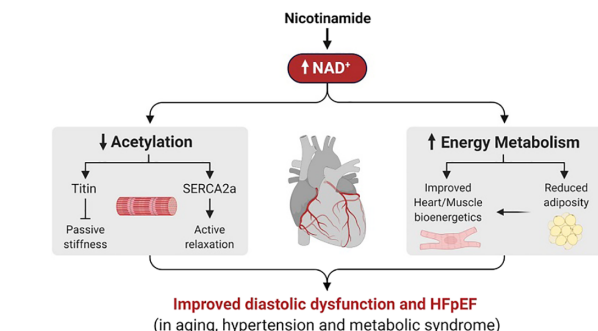
**Funding Acknowledgements:** Minotaur Consortium, ERA-CVD

**Rationale:** Heart failure with preserved ejection fraction (HFpEF) is a highly prevalent and intractable form of cardiac decompensation commonly associated with diastolic dysfunction. Experimentally, HFpEF is intimately linked to metabolic perturbations in mitochondrial fatty acid oxidation, redox reactions, and ATP synthesis. Since all these processes are nicotinamide adenine dinucleotide (NAD<sup>+</sup>)-dependent, we hypothesized that NAD<sup>+</sup> metabolism is deranged in HFpEF and, thus, it might be therapeutically targeted.

**Methods:** To induce local NAD<sup>+</sup> deficiency, we generated mice with partial deletion of nicotinamide phosphoribosyltransferase (NAMPT) specifically in cardiomyocytes. We also used ZSF1 obese rats as a model of metabolic syndrome-induced HFpEF, whereas 2-year-old C57BL6/J mice and Dahl salt-sensitive rats were employed to examine age- and hypertension-related diastolic dysfunction, respectively. We applied a multitude of in vivo and in vitro assays, including invasive hemodynamics, serial echocardiography and blood pressure measurements, exercise tolerance testing, indirect calorimetry, cardiac acetylome and metabolome profiling, myocardial and skeletal muscle bioenergetics. Synchronized calcium photometry and sarcomere shortening measurements, and titin mechanics were performed in isolated cardiomyocytes. The translational potential of the study was examined in cardiac biopsies of HFpEF and non-failing donors, and in a human cohort with 20 years of follow-up.

**Results:** HFpEF in patients and ZSF1 obese rats was associated with a cardiac decline in NAD<sup>+</sup> levels. Mimicking NAD<sup>+</sup> deficiency in mice, by local NAMPT haploinsufficiency, caused premature diastolic dysfunction. Contrarily, elevating NAD<sup>+</sup> levels by oral supplementation of its precursor, nicotinamide, improved diastolic dysfunction induced by metabolic syndrome, salt-sensitive hypertension or old age. This effect was mediated partly through alleviated systemic comorbidities and enhanced myocardial bioenergetics. Simultaneously, nicotinamide directly improved cardiomyocyte passive stiffness and calcium-dependent active relaxation through increased deacetylation of titin and SERCA2a, respectively. Finally, in a long-term human cohort study, high dietary intake of naturally-occurring NAD<sup>+</sup> precursors was associated with lower blood pressure and reduced risk of cardiac and all-cause mortality.

**Conclusion:** NAD<sup>+</sup> precursors, and especially nicotinamide, hold promise as potential therapeutic agents against diastolic dysfunction and clinical HFpEF.



Mechanistic model

### Effects of renal sympathetic denervation on the course of CHF combined with chronic kidney disease: insight from studies with fawn-hooded hypertensive rats with aorto-caval fistula

Z Honetschlagerova<sup>1</sup>; P Skaroupkova<sup>1</sup>; S Kikerlova<sup>1</sup>; Z Huskova<sup>1</sup>; H Maxova<sup>2</sup>; V Melenovsky<sup>1</sup>; E Kompanowska-Jezierska<sup>3</sup>; J Sadowski<sup>3</sup>; O Gawrys<sup>1</sup>; L Cervenka<sup>1</sup>; <sup>1</sup>Institute for Clinical and Experimental Medicine (IKEM), Prague, Czechia; <sup>2</sup>Charles University of Prague, Second Faculty of Medicine, Prague, Czechia; <sup>3</sup>Mossakowski Medical Research Centre, Warsaw, Poland;

**Funding Acknowledgements:** Ministry of Health of the Czech Republic grant no. nu 20-02-00052 awarded to L.C. and V.M.

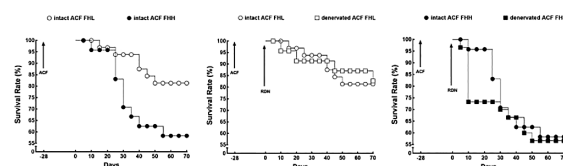
**Introduction:** Coincidence of congestive heart failure (CHF) and chronic kidney disease (CKD) results in poor survival rate, therefore new therapeutic approaches are needed.

**Objective:** The aim of the study was to examine if renal denervation (RDN) would improve the survival rate in CHF induced by creation of aorto-caval fistula (ACF).

**Methods:** This was studied in fawn-hooded hypertensive rats (FHH), a genetic model showing CKD development. Fawn-hooded low-pressure rats (FHL), without CKD, served as controls. RDN was performed four weeks after creation of ACF and the follow-up period was 10 weeks.

**Results:** We found that intact (non-denervated) ACF FHH exhibited survival rate of 58.8% (20 of 34 rats), significantly lower than in intact ACF FHL (81.3%, 26/32 rats). In intact ACF FHL rats albuminuria remained stable throughout the study whereas in ACF FHH it increased significantly, up to a level 40-fold higher than the basal values. RDN did not improve the survival rate in either ACF FHL or ACF FHH and did not alter the course of albuminuria in ACF FHL. In contrast, RDN attenuated the rise in albuminuria in ACF FHH and at the end of the study it was about 40% lower than in intact ACF FHH.

**Conclusions:** Our present results support the notion that even modest CKD increases CHF-related mortality. While RDN did not attenuate CHF-dependent mortality in ACF FHH, it delayed the progressive rise in albuminuria, suggesting that renal denervation could be a novel therapeutic measure for the treatment of CHF, particularly the form associated with CKD.



Survival rates

### Effect of epoxyeicosatrienoic acid analogue alone or combined with angiotensin-converting enzyme inhibitor on the course of congestive heart failure induced by aorto-caval fistula in hypertensive rats

P Kala<sup>1</sup>; P Skaroupkova<sup>2</sup>; Z Honetschlagerova<sup>2</sup>; M Miklovic<sup>2</sup>; V Melenovsky<sup>2</sup>; J Veselka<sup>1</sup>; L Cervenka<sup>2</sup>; <sup>1</sup>Motol University Hospital, Prague, Czechia; <sup>2</sup>Institute for Clinical and Experimental Medicine (IKEM), Prague, Czechia;

**Funding Acknowledgements:** Charles University Grant Agency, grant no. 32218 awarded to P.K.

**Introduction:** The long-term prognosis of patients with congestive heart failure (CHF) remains poor, thus new therapeutic strategies for the treatment are needed. The current knowledge suggest that targeting the eicosanoid system could be a promising approach. Absolute or relative lower plasma and organ levels of epoxyeicosatrienoic acids (EET) might contribute to progression of CHF.

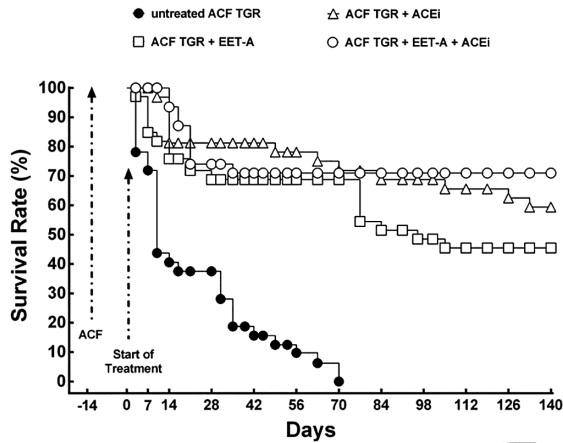
**Purpose:** To examine if chronic treatment by epoxyeicosatrienoic acid analogue (EET-A) would attenuate the course of CHF induced by volume overload achieved by creation of the aorto-caval fistula (ACF).

**Methods:** In Ren-2 transgenic rats (TGR), a model of angiotensin II-dependent hypertension, chronic treatment by EET-A was achieved by 14,15-EET analogue (100 mg.L<sup>-1</sup> in drinking water, i.e. 10 mg.kg<sup>-1</sup>.day), and its effect on the CHF-related mortality was compared with angiotensin-converting enzyme inhibitor (ACEi) (trandolapril, 2 mg.L<sup>-1</sup> in drinking water) and combined therapy by EET-A + ACEi (14,15-EET analogue, 100mg.L<sup>-1</sup> and trandolapril, 2 mg.L<sup>-1</sup> in drinking water). ACF was created at the animal age of 8 weeks, 2 weeks later the animals were randomly divided into 4 groups and the therapy began (EET-A n=31, ACEi n=32, EET-A + ACEi n=32 or placebo n=30). Sham-operated TGR represented a control group (n=8). The follow-up period was 20 weeks. GraphPad Prism 7 was used for statistical analysis with log-rank (Mantel-Cox) test for analysis of survival data.

**Results:** All sham-operated rats survived till the end of study. Untreated CHF rats began to die at the week 3 after creation of ACF and all the animals died by the

week 12. The treatment with the EET-A or with ACEi similarly improved the survival rate, and the final rate was 45 % in EET-A group (14 of 31 rats; vs. placebo  $P < 0.01$ ) and 62 % in ACEi group (20 of 32 rats; vs. placebo  $P < 0.01$ ), with non-significant intergroup difference – ACEi vs. EET-A,  $P = 0.09$ ). Combined therapy by EET-A + ACEi improved survival similarly with the final rate 72% (23 of 32, vs. placebo and EET-A  $P < 0.01$ , a non-significant trend vs. ACEi). In ACF TGR all therapeutic regimes reduced albuminuria, significantly below the level observed in sham-operated TGR.

**Conclusion:** Our results suggest that in ACF TGR the treatment with EET analogue markedly attenuates CHF-dependent mortality and reduces albuminuria, both to the same extent as with ACEi treatment, however combination treatment by EET-A and ACEi did not showed significant additional improvement in survival over ACEi alone.



Survival rate

#### Statin is associated with lower cancer risk and cancer related mortality in patients with heart failure: a territory-wide study

QW Qingwen Ren<sup>1</sup>; SY Yu<sup>2</sup>; X Li<sup>1</sup>; KS Cheung<sup>1</sup>; MZ Wu<sup>1</sup>; HL Li<sup>2</sup>; PF Wong<sup>1</sup>; HF Tse<sup>1</sup>; Sp Lam<sup>3</sup>; KH Yiu<sup>1</sup>; <sup>1</sup>Queen Mary Hospital, Hong Kong, Hong Kong; <sup>2</sup>The University of Hong Kong, Hong Kong, China; <sup>3</sup>National Heart Centre Singapore, Singapore, Singapore;

**Funding Acknowledgements:** None

**Background:** Patients with heart failure (HF) is associated with a high risk of cancer. The effect of statin use among patients with HF on cancer risk and cancer-related mortality is nonetheless unknown.

**Methods:** Using a territory-wide clinical information registry, statin use was ascertained among all eligible patients with HF (N = 87 102) from 2003 to 2015. Inverse probability of treatment weighting was used to balance baseline covariates between statin nonusers (50 926 patients) with statin users (36 176 patients). Competing risk regression with Cox proportional-hazard models was performed to estimate the risk of cancer and cancer-related mortality associated with statin use.

**Results:** Of all eligible subjects, 11 052 (12.7%) were diagnosed with cancer. Statin use was associated with a 16% lower risk of cancer incidence (multivariable adjusted subdistribution hazard ratio [SHR]=0.84; 95% Confidence Interval [CI], 0.80 to 0.89). This inverse association with risk of cancer was duration-dependent; as compared with short-term statin use (3 months to <2 years), the adjusted SHR were 0.99 (95% CI, 0.87 to 1.13) for 2 to less than 4 years of use, 0.82 (95% CI, 0.70 to 0.97) for 4 to less than 6 years of use, and 0.78 (95% CI, 0.65 to 0.93) for 6 or more years of use. Ten-year cancer-related mortality was 3.8% among statin users and 5.2% among nonusers (absolute risk difference, -1.4 percentage points [95% CI, -1.6% to -1.2%]; adjusted SHR=0.74; 95% CI, 0.67 to 0.81).

**Conclusions:** Our study suggests that statin use is associated with a significantly lower risk of cancer incident and cancer-related mortality and appears to be duration-dependent.

#### History of heart failure in COVID-19 patients: insights from a French registry

V Panagides<sup>1</sup>; F Vincent<sup>2</sup>; O Weizman<sup>3</sup>; M Jonveaux<sup>4</sup>; A Trimaille<sup>5</sup>; T Pommier<sup>6</sup>; J Cellier<sup>7</sup>; B Ducau<sup>8</sup>; W Sutter<sup>9</sup>; D Mika<sup>9</sup>; T Pezel<sup>10</sup>; V Waldmann<sup>7</sup>; J Ternacle<sup>11</sup>; A Cohen<sup>12</sup>; G Bonnet<sup>11</sup>; <sup>1</sup>APHM LA TIMONE HOSPITAL, Cardiology, Marseille, France; <sup>2</sup>Chru De Lille - Institut Coeur-Poumons, Cardiology, Lille, France; <sup>3</sup>University Hospital of Nancy, Cardiology, Nancy, France; <sup>4</sup>Mondor Hospital, Cardiology, Paris, France; <sup>5</sup>University Hospital of Strasbourg, Cardiology, Strasbourg, France;

<sup>6</sup>University Hospital of Dijon, Dijon, France; <sup>7</sup>European Hospital Georges Pompidou, Cardiology, Paris, France; <sup>8</sup>Paris Cardiovascular Research Center (PARCC), Paris, France; <sup>9</sup>Inserm, UMR-S 1180, Paris, France; <sup>10</sup>Hospital Lariboisiere, Cardiology, Paris, France; <sup>11</sup>University Hospital of Bordeaux, Cardiology, Bordeaux, France; <sup>12</sup>Hospital Saint-Antoine, Cardiology, Paris, France;

**On behalf of:** Critical COVID-19 France Investigators

**Funding Acknowledgements:** NCT04344327

**Background:** Data concerning COVID-19 patients with pre-existing heart failure are scarce.

**Aims:** To investigate the incidence, characteristics and outcomes of COVID-19 patients with a history of heart failure (HF) with preserved (HFpEF) or reduced (HFrEF) ejection fraction.

**Methods:** All patients hospitalized for COVID-19 across 24 centres in France were included from February 26 to April 20, 2020. Primary endpoint was a composite of in-hospital death or orotracheal intubation.

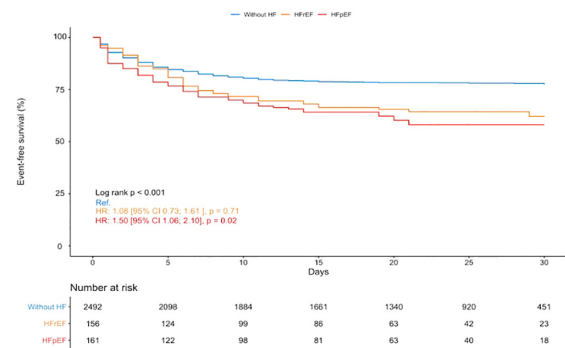
**Results:** Of 2809 patients ( $66.4 \pm 16.9$  years), 317 patients (11.2%) had a history of HF. Among them, 49.2% had HFrEF and 50.8% had HFpEF. COVID-19 severity at admission, defined by a quick sequential organ failure (qSOFA) score >1, was similar in patients with versus without a history of HF. Before and after adjustment for age, sex, male, cardiovascular comorbidities and qSOFA score, history of HF was associated with the primary endpoint (hazard ratio (HR) 1.41; 95% confidence interval (CI): 1.06;1.90,  $P = 0.02$ ). This result seemed to be mainly driven by history of HFpEF (HR 1.61; 95%CI: 1.13;2.27,  $P = 0.01$ ) versus HFrEF (HR 1.19; 95%CI: 0.79;1.81,  $P = 0.41$ ).

**Conclusions:** History of HF in COVID-19 patients was associated with a higher risk of in-hospital death or orotracheal intubation, suggesting that they are at increased risk for clinical deterioration.

#### Multivariate analysis

	Hazard Ratio	95% CI	P-value
Global HF model			
Age	1.01	1.01;1.02	< 0.001
Male	1.58	1.28;1.95	< 0.001
Body mass index	1.02	1.00;1.03	0.06
Hypertension	1.08	0.82;1.43	0.57
Diabetes	1.34	1.07;1.68	0.01
Coronary artery disease	0.84	0.62;1.15	0.28
Stroke	0.92	0.67;1.26	0.60
Chronic kidney disease	1.51	1.17;1.95	< 0.001
Global HF	1.41	1.06;1.90	0.02
RAAS inhibitors	0.96	0.75;1.22	0.72
Beta-blockers	0.90	0.70;1.16	0.40
qSOFA score	2.10	1.68;2.64	< 0.001

HF denotes Heart Failure; qSOFA, Quick Sepsis-related Organ failure Assessment; RAAS, renin-angiotensin-aldosterone system inhibitors



Kaplan-Meier curves

## Ketone bodies improve myocardial function in heart failure

J Gambardella<sup>1</sup>; S Jankauskas<sup>2</sup>; M Morelli<sup>3</sup>; XJ Wang<sup>3</sup>; G Santulli<sup>2</sup>; <sup>1</sup>University Hospital Federico II, Naples, Italy; <sup>2</sup>Albert Einstein College of Medicine at Montefiore Hospital, The Bronx, USA; <sup>3</sup>Albert Einstein College of Medicine, The Bronx, USA;

**Funding Acknowledgements:** None

**Background:** Beta hydroxybutyrate (BHB) is the main ketone body produced during fasting or carbohydrate deprivation as an alternative fuel. Mounting evidence suggests that after myocardial infarction (MI), mitochondrial impairment and metabolic failure coincide with increased levels and utilization of BHB. However, whether the observed increase in BHB is adaptive or maladaptive in damaged myocardium, has never been evaluated.

**Aim:** Our main scope was to explore the effects of BHB on cardiac function after ischemia both in vivo and in vitro.

**Methods and Results:** In cultured cardiomyoblasts, the administration of BHB (3 mM) reduces the activation of caspase-3 in response to ischemia, as well as the number of tunnel positive nuclei. Specifically, the mitochondrial apoptotic pathway seems affected, as BHB reduces cytochrome-C release induced by ischemia. Mitochondrial structure and interconnections, soundly affected by ischemia, were significantly retained in presence of BHB, as well as mitochondrial membrane potential (assessed via TMRE). The preserved mitochondrial health was further supported by higher levels of PGC1- $\alpha$  detected in cells exposed to ischemia plus BHB compared to ischemia alone. To explore the in vivo effects of BHB on ischemia damaged- myocardium, we administered carbohydrate-null diet (ketogenic diet, KD) or standard diet-supplemented with BHB, to post-MI mice. Both groups treated with KD and BHB supplemented diet displayed preserved left ventricular ejection fraction respect to untreated infarcted mice. The protective effects of BHB on cardiac phenotype were mirrored by increased levels of PGC1- $\alpha$  in the myocardium of treated mice, in terms of protein and transcription levels. Interestingly, in the hearts of mice fed KD and BHB supplemented diet, we observed a marked difference in histone acetylation pattern.

**Conclusions:** BHB protects cardiac cells from apoptotic and mitochondrial damage induced by ischemia. Through its ability to regulate epigenetic modifications, BHB could activate a gene expression program able to support mitochondrial function, thereby representing a powerful therapeutic strategy.

## Myocardial Disease – Pathophysiology and Mechanisms

### M1/M2 ratio predicts cardiac systolic function after myocardial infarction with ST elevation (STEMI)

E De Angelis<sup>1</sup>; MR Rusciano<sup>2</sup>; I Radano<sup>1</sup>; A Silverio<sup>1</sup>; R Citro<sup>1</sup>; A Ravera<sup>1</sup>; P Di Pietro<sup>1</sup>; A Carrizzo<sup>2</sup>; C Vecchione<sup>1</sup>; G Galasso<sup>1</sup>; M Ciccarelli<sup>1</sup>; <sup>1</sup>University of Salerno School of Medicine, Cardiology Unit, Cardiovascular and Thoracic Department, Salerno, Italy; <sup>2</sup>University of Salerno School of Medicine, Department of Medicine, Surgery and Odontology, Salerno, Italy;

**Funding Acknowledgements:** None

**Background:** In response to myocardial infarction (MI), cardiac monocytes and macrophages regulate inflammation and scar formation playing a crucial role in infarct healing and subsequent LV remodelling. In humans, two different monocyte subsets are identified: classical CD14<sup>++</sup>CD16<sup>-</sup>, so-called M1 monocytes and non-classical CD14<sup>++</sup>CD16<sup>++</sup> or M2 monocytes; these two populations show a different pro-inflammatory activity. The prognostic impact of monocyte subsets post-ST elevation myocardial infarction (STEMI) remains, nonetheless, unknown.

**Purpose** In this study, we sought to examine the dynamic changes of the 2 monocyte subsets in a contemporary population with anterior STEMI and correlate these changes with the short-term cardiovascular outcome.

**Methods** We enrolled prospectively 64 patients with a diagnosis of anterior STEMI, with total ischemic time inferior to 4 h. Levels of classical and nonclassical peripheral monocytes were evaluated by FACS analysis at hospital admission (time 0), 48 and 96 h post-admission.

After 96 h from admission all patients underwent a cardiac echography for the evaluation of cardiac volumes, left ventricular ejection fraction (LVEF) and left ventricular global longitudinal strain; patients were divided into two groups according to the LVEF (LVEF < 45% and LVEF  $\geq$  45%).

**Results** Baseline characteristics, pharmacological treatment, total ischemia time and post-PCI TIMI flow did not show significative differences with the exceptions of diuretics use that was prevalent in the LVEF < 45% population (20% n=4 in LVEF < 45%; n=0 in LVEF  $\geq$  45%;  $P=0.001$ ), cardiac arrest (20% n=4 in LVEF < 45%; n=0 in LVEF  $\geq$  45%;  $P=0.001$ ), and ventricular fibrillation (20% n=4 in LVEF < 45%; n=0 in LVEF  $\geq$  45%;  $P=0.001$ ). Total peripheral monocyte counts were not different between the two populations at the three timepoint ( $P=0.486$  a T0;  $P=0.213$  a T48;  $P=0.456$  a T96). However, M1 monocytes were significantly increased at T0, T48 and T96 in the LVEF < 45% (T0: 63.8%, T48: 60%, T96: 55.8%) than the LVEF  $\geq$  45% population (T0: 37%, T48: 43.7%, T96: 62%;  $P<0.000$ ). Also

M2 monocytes were significantly increased at T0, T48 and T96 in the LVEF < 45% (T0: 85%, T48: 98%, T96: 91%) than the LVEF  $\geq$  45% (T0: 67%, T48: 44.9%, T96: 36.9%;  $P=0.005$  for T0,  $P=0.002$  for T48,  $P<0.000$  for the T96). The T48 and T96 M1/M2 ratio was reduced in the LVEF < 45% group. Moreover, the M1/M2 ratio at 48 and 96 h presented a significant positive linear correlation with the LVEF ( $R=0.063$  at T0,  $P=0.272$ ;  $R=0.128$  at T48,  $P=0.016$ ;  $R=0.316$  at T96,  $P=0.001$ ) confirmed by the logistic regression (OR = 1.646 at T0,  $P=0.419$ ; OR = 4.339 at T48,  $P=0.035$ ; OR = 4.635 at T96,  $P=0.014$ ).

**Conclusions:** In summary, elevation of M2-monocytes and a lower M1/M2 ratio are related to a reduced LVEF possibly due to a pronounced pro-fibrotic state. Our data demonstrate that M1 and M2 monocytes expression can predict the outcome of the systolic cardiac function in a short time after STEMI.

### Targeting GRK2 to prevent aortic valve calcification

M Rusciano<sup>1</sup>; D Sorriento<sup>2</sup>; G Iaccarino<sup>2</sup>; P Poggio<sup>3</sup>; M Ciccarelli<sup>1</sup>; <sup>1</sup>University of Salerno, Department of Medicine, Surgery and Odontology, Salerno, Italy; <sup>2</sup>Federico II University Hospital, Advanced Biomedical Sciences, Naples, Italy; <sup>3</sup>Centro Cardiologico Monzino, IRCCS, Unità per lo Studio delle patologie Aortiche, Valvolari e Coronariche, Milan, Italy;

**Funding Acknowledgements:** None

**Background:** Calcific aortic valve stenosis (CAVS) is a clinically relevant issue due to the lack of drugs for prevention or treatment. CAVS is driven by endothelial dysfunction and inflammation. A novel therapeutic strategy should target specific molecules involved in the regulation of both endothelial function and immune responses. G protein-coupled receptor kinase 2 (GRK2) regulates desensitization and downregulation of G protein-coupled receptors, but more recently, it has been shown to interact with an extensive repertoire of proteins. We previously demonstrated that the lack of this protein in the endothelium promotes vascular inflammation and atherosclerosis in mice due to increased mitochondrial reactive oxygen species (ROS).

**Purpose:** This study aimed to evaluate the role of GRK2 in Aortic Valve Calcification (AVC) by in vivo and in vitro studies.

**Methods:** To reach our purpose we evaluated GRK2 expression in mitochondria isolated from the valve of patients with calcified (CAVS) aortic valve leaflets vs. control ECs. We also performed histological analysis by using 12 months old mice with selective endothelial knock-out of GRK2 (Tie2CRE-GRK2fl/fl) in EC compared to control (GRK2fl/fl) to evaluate the presence of microcalcification in the aortic valve. Finally, we cloned a small sequences of the PH domain of  $\beta$ ARKct into the pcDNA3 to induce GRK2 localization into mitochondria.

**Results:** In vitro, we observed a significant downregulation of GRK2 expression into the mitochondria of CAVS VECs than control VECs, which associates to an increased ROS production. Histological analysis revealed that GRK2fl/fl mice of 12 months-old display presence of microcalcification, as expected. However, this phenotype is significantly more pronounced in the Tie2CRE-GRK2fl/fl, demonstrating that the lack of GRK2 in the EC accelerates the calcific degeneration of the aortic valve in mice. A previous report demonstrated that  $\beta$ ARKct transfection in macrophage increases mitochondrial biogenesis and reduces ROS production. Here, we cloned several small sequences of the PH domain of  $\beta$ ARKct into the pcDNA3.1 plasmid, named as PH#1-4. We found that the transfection into HEK293 cells of the PH#3 potently increased GRK2 localization into the mitochondria as compared to  $\beta$ ARKct, PH4, and pcDNA3.1 as control. PH3 also determined increased biogenesis and reduced ROS production after AngII stimulation. These data support the concept that a smaller portion of the PH domain of  $\beta$ ARKct can reproduce its biological effect.

**Conclusions:** In conclusion, our data suggest a direct involvement of GRK2 expression/localization in the pathogenesis of CAVS. Intracellular re-localization of GRK2 could be a novel strategy to prevent AVC in a pathophysiological condition such as ageing

### Microarray analysis to identify potential biomarkers in adverse cardiac remodeling in patients with myocardial infarction: pilot study

A Aleksandra Gombozhapova<sup>1</sup>; Y Rogovskaya<sup>1</sup>; N Litvyakov<sup>2</sup>; M Ibragimova<sup>2</sup>; I Lariionova<sup>3</sup>; J Kzhyskowska<sup>4</sup>; V Ryabov<sup>1</sup>; <sup>1</sup>Cardiology Research Institute, Tomsk NRMC, Tomsk, Russian Federation; <sup>2</sup>Tomsk Cancer Research Institute, Tomsk, Russian Federation; <sup>3</sup>National Research Tomsk State University, Tomsk, Russian Federation; <sup>4</sup>University of Heidelberg, Heidelberg, Germany;

**Funding Acknowledgements:** None

**Introduction:** The mechanism of adverse cardiac remodeling following myocardial infarction (MI) remains unclear. It consists of variety of changes at different biological levels. Transcriptome is one of the most intriguing levels. Nowadays we have series of transcriptome databases with experimental data on post-infarction cardiac remodeling. Obviously, not all experimental data can be extrapolated to the clinical studies. The response to ischemic injury in the infarct zone and remote myocardium

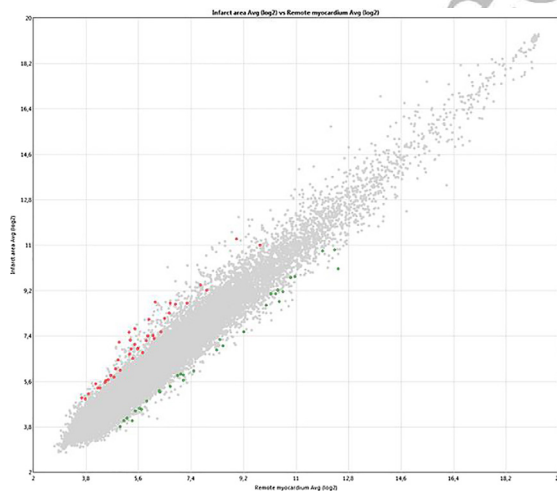
has a definite spatio-temporal sequence and underlies the mechanism of cardiac remodeling. However, potential differences in gene expression between the infarct zone and remote myocardium in patients with MI are not investigated yet.

**Purpose:** The purpose of the research was to identify the differentially expressed genes (DEGs) between the infarct zone and remote myocardium in patients with MI.

**Methods:** The study included 4 patients with fatal MI type 1. All patients died within 48 h of MI. The post-mortem examination was performed according to country policy. In each case, we obtained myocardial samples from the infarct zone and remote myocardium. Genome-wide gene-level expression was assessed by microarray analysis. We used transcriptome analysis software to analyze and visualize global expression patterns of genes. DEGs were defined as gene-level fold change  $< -2$  or  $> 2$  and adjusted  $P$ -value of  $< 0.05$ .

**Results:** We studied expression of 21448 genes. A total of 71 DEGs, including 41 up-regulated genes and 31 down-regulated genes, were identified (Figure 1). Up-regulated genes included FCGR2C, DTNA, BMP5, FGFR1OP, TRAFD1, PLCB1, PRDM1, SELE, PLP1, ANKRD13A, MTA3, ATP6V0C, MMS22L, ATXN1, STAT4, RAD51B, TRMT10A, TMEM133, ATP8A1, C3orf38, GPR34, ITGA8, VAMP8, CUEDC2, AP1AR, C9orf85, PECR, TSPYL2, SORBS1, CGNL1, FRMD6, GRK4, CYT1, TTC30B, DOCK2, FGF4, KLRC3, SLITRK6, DNAJC5G, CADM2, SNIP1. Down-regulated genes included FAM84B, PLS1, CAMK1, SWI5, CYP2S1, CRB3, ULBP1, RBPMS2, GTF2F1, MCRS1, IMP3, CCDC121, CARM1, PHLPP2, OR10G8, NAA16, MYH9, PRELID1, NPM3, GGT5, HAGH, USP6, SUSD6, HYOU1, MIR4658, BCL7C, TTC7B, ADSSL1, HYOU1, RCAN1, COBL. The most significantly up-regulated genes in the infarct zone were FCGR2C, DTNA, BMP5, while the most significantly down-regulated gene were HYOU1, RCAN1, and COBL. Our analysis revealed that up-regulated DEGs were mainly enriched in the platelet activation and aggregation pathways, in cyclooxygenase pathway, in chemokine signaling pathway, in negative regulation of mononuclear cell migration, in neurons necrosis caused by energy deficiency, in positive regulation of extracellular matrix disassembly, in positive regulation of mast cell degranulation.

**Conclusion:** The results of our pilot study have demonstrated differences in gene expression between the infarct zone and remote myocardium in clinical settings. Following steps of our research can include bioinformatics analysis and validation process.



DEGs: red - up-reg, green - down-reg

#### MicroRNAs drive endothelial dysfunction and thromboembolism in COVID-19

J Gambardella<sup>1</sup>; M Morelli<sup>2</sup>; C Sardu<sup>3</sup>; p Maggi<sup>3</sup>; A Matarese<sup>4</sup>; R Marfella<sup>3</sup>; V Messina<sup>3</sup>; S Jankauskas<sup>2</sup>; G Paolisso<sup>3</sup>; G Gaetano Santulli<sup>1</sup>; <sup>1</sup>University Hospital Federico II, Naples, Italy; <sup>2</sup>Albert Einstein College of Medicine, The Bronx, USA; <sup>3</sup>Vanvitelli University, Naples, Italy; <sup>4</sup>AO dei Colli-Monaldi Hospital, Naples, Italy;

**Funding Acknowledgements:** None

**Background:** Thromboembolic complications play a crucial role in the clinical outcome of COVID-19. Emerging evidence has shown that exosomal microRNAs (miRNAs) are functionally involved in several pathologic processes. In March 2020, we were the first group to functionally link COVID-19 and endothelial dysfunction.

**Methods:** To test the hypothesis that exosomal miRNAs are a key determinant of thrombosis in COVID-19, we enrolled 26 COVID-19 patients. The study was approved by the local Ethical Committees. Circulating exosomes were isolated as we previously described and validated by our group and levels of exosomal miRNAs,

from a custom panel of miRNAs, were quantified by RT-qPCR and normalized to the expression of U18.

**Results:** We divided our population in two groups based on serum D-dimer level on admission, using a previously published cut-off of  $3 \mu\text{g/ml}$ . No significant differences in the main clinical characteristics were noted comparing patients with low ( $n=11$ ) vs. high ( $n=15$ ) D-Dimer. Strikingly, we found that exosomal miR-424 was significantly upregulated whereas exosomal miR-103a, miR-145, and miR-885 were significantly downregulated in patients in the high D-dimer group compared to patients in the low D-Dimer group ( $P < 0.0001$ ). Regression analysis confirmed these findings. Mechanistically, Tissue Factor (TF) was identified as a direct target of miR-145, while miR-885 targets the von Willebrand Factor (vWF). Equally important, miR-424 has been associated with hyper-coagulability whereas low levels of miR-103a have been observed in deep vein thrombosis, although precise mechanisms have not been defined for these miRNAs. Using a stepwise multiple regression analysis, exosomal miR-424 was an independent predictor of thromboembolic events (i.e. pulmonary embolism and acute myocardial infarction) in COVID-19 patients (Wald: 4.180;  $P < 0.05$ ), whereas miR-103a independently regulated D-dimer levels ( $P < 0.001$ ).

**Conclusions:** To our knowledge, this is the first study showing a significant contribution of exosomal non-coding RNAs in COVID19. Limitations of our study include the relatively small population and the fact that we did not determine the exact source of exosomes; nevertheless, we speculate that a main source could be represented by endothelial cells and/or platelets, which express these miRNAs in normal conditions.

## Basic Science – Cardiac Biology and Physiology

### Mechano-energetic uncoupling underlies lack of inotropic reserve in Barth syndrome cardiomyopathy

E Bertero<sup>1</sup>; A Nickel<sup>1</sup>; M Kohlhaas<sup>1</sup>; M Hohl<sup>2</sup>; V Sequeira<sup>1</sup>; J Schwemmlin<sup>1</sup>; C Carlein<sup>3</sup>; A Mueller<sup>4</sup>; K Von Der Malsburg<sup>5</sup>; M Van Der Laan<sup>5</sup>; P Rehling<sup>6</sup>; L Prates-Roma<sup>3</sup>; J Dudek<sup>1</sup>; C Maack<sup>1</sup>; <sup>1</sup>University Clinic Würzburg, Comprehensive Heart Failure Center, Würzburg, Germany; <sup>2</sup>Saarland University Clinic, Clinic for Internal Medicine III, Homburg/Saar, Germany; <sup>3</sup>Saarland University, Department for Biophysics, Homburg/Saar, Germany; <sup>4</sup>Saarland University Clinic, Clinic for Radiology, Homburg/Saar, Germany; <sup>5</sup>Saarland University, Medical Biochemistry and Molecular Biology, Homburg/Saar, Germany; <sup>6</sup>Georg-August University, Department of Cellular Biochemistry, Goettingen, Germany;

**Funding Acknowledgements:** German Research Foundation (DFG); Barth Syndrome foundation (BSF)

**Background:** Barth syndrome (BTHS) is an X-linked disorder characterized by cardiomyopathy, skeletal myopathy, and delayed growth. BTHS is caused by mutations in the tafazzin gene (Taz), which encodes an enzyme involved in the biosynthesis of cardiolipin, a mitochondrial phospholipid. We previously discovered that the mitochondrial calcium (Ca<sup>2+</sup>) uniporter (MCU) requires cardiolipin, and thereby BTHS leads to a cardiac-specific defect in mitochondrial Ca<sup>2+</sup> uptake. Here, we investigated the consequences of cardiolipin deficiency and MCU loss on cardiac mechano-energetic coupling in a mouse model of BTHS (Taz-knockdown mice).

**Methods and Results:** To investigate the mechanisms underlying cardiomyopathy in Taz-KD mice, we analyzed mitochondrial redox state (by NAD(P)H and FAD autofluorescence), cellular contractility, and cytosolic Ca<sup>2+</sup> handling in isolated, field-stimulated cardiac myocytes. In Taz-KD myocytes, defective mitochondrial Ca<sup>2+</sup> accumulation hindered the Ca<sup>2+</sup>-induced regeneration of NAD(P)H and FADH<sub>2</sub> by the Krebs cycle, leading to oxidation of mitochondrial redox state during combined  $\beta$ -adrenergic and 5 Hz stimulation. Inhibition of the mitochondrial sodium/Ca<sup>2+</sup> exchanger, which mediates Ca<sup>2+</sup> efflux from mitochondria, partially rescued mitochondrial oxidation and prevented spontaneous (non-stimulated) contractions observed in Taz-KD, but not wild-type (WT) myocytes. Taz-KD cardiac myocytes displayed enhanced contractility and shorter diastolic sarcomere length compared to WT at baseline (0.5 Hz pacing). However, diastolic cytosolic Ca<sup>2+</sup> levels ([Ca<sup>2+</sup>]<sub>i</sub>) and amplitude of Ca<sup>2+</sup> transients did not differ between genotypes. Furthermore, although the rate of [Ca<sup>2+</sup>]<sub>i</sub> decay was markedly faster than WT, Taz-KD myocytes exhibited prolonged kinetics of sarcomere re-lengthening that progressed between 10 and 50 weeks of age. Combined  $\beta$ -adrenergic and 5 Hz stimulation increased sarcomere shortening in WT and Taz-KD myocytes, but this was not accompanied by an increase in cytosolic Ca<sup>2+</sup> transient amplitude in Taz-KD myocytes. When assessing the force-Ca<sup>2+</sup> relationship of membrane-permeabilized and mechanically preloaded myocytes, Taz-KD myocytes developed more force than WT at any Ca<sup>2+</sup> concentration, indicating higher myofilament Ca<sup>2+</sup> sensitivity. In mechanically prestretched myocytes, the frequency-dependent potentiation of force development observed in WT was absent and even negative in Taz-KD cardiac myocytes.

**Conclusions:** Disruption of the mechano-energetic coupling reserve is a primary defect in BTHS cardiomyopathy. Impaired bioenergetic adaptation due to deficient mitochondrial Ca<sup>2+</sup> uptake is accompanied by maximal recruitment of cardiac inotropic and lusitropic reserve, preventing the physiological increase in contractility during elevations of workload. These data provide mechanistic insights into two

major clinical problems in BTHS, i.e., the inability of the heart to increase contractility during exercise and the increased risk of arrhythmias.

#### TMEM43 mutation p.S358L results in changes in cardiac morphology and performance in transgenic zebrafish

M Miriam Zink<sup>1</sup>; A Seewald<sup>1</sup>; M C Nguyen<sup>1</sup>; T Williams<sup>1</sup>; D Liedtke<sup>2</sup>; C Stigloher<sup>2</sup>; S Childs<sup>3</sup>; B Gerull<sup>1</sup>; <sup>1</sup>University Hospital Wuerzburg, Wuerzburg, Germany; <sup>2</sup>University of Wuerzburg, Wuerzburg, Germany; <sup>3</sup>University of Calgary, Calgary, Canada;

**Funding Acknowledgements:** Grant number 01EO1504, Federal Ministry of Education and Research, Germany (BMBF)

**Background:** Arrhythmogenic cardiomyopathy (ACM) is an inherited heart muscle disorder, predisposing to arrhythmias, heart failure and sudden cardiac death. A fully penetrant heterozygous missense mutation c.1073C>T (p.S358L) within the highly conserved gene of transmembrane protein 43 (TMEM43) has been genetically identified to cause a severe subtype of ACM. A second variant (c.332C>T; p.P111L) within TMEM43 has not been functionally validated yet. TMEM43 is an integral protein of the inner nuclear membrane and is involved in maintaining the structural integrity of the nuclear envelope.

**Methods and Results:** We generated cardiomyocyte-restricted transgenic zebrafish lines that overexpress eGFP-linked full-length human wildtype TMEM43 and the respective mutations using the Tol2-system. Mutant transgenic zebrafish are viable and survive until adulthood. At 72 h post fertilisation cardiac phenotyping of the F3 incross generation revealed an elevated percentage of cardiac developmental defects in TMEM43 mutant zebrafish larvae. Furthermore, both TMEM43 mutant zebrafish lines showed a decreased end-diastolic and end-systolic ventricular area. However, the overall ventricular contractility was enhanced, indicated by increased fractional shortening and fractional area change values. Moreover, the contractions appeared to be much more heterogenous with hypercontractility localised at certain areas of the ventricle. To identify the reason for the smaller ventricular size, whole-mount immunofluorescence (IF) staining unveiled a significantly reduced cross-sectional area of the ventricular cardiomyocytes in the p.S358L-mutant zebrafish. As the mean nuclear area was also smaller, the nuclear-cytoplasmic ratio remained unchanged, as well as the number of overall nuclei. This leads to the hypothesis that pathways involved in growth and proliferation are potentially affected. To analyse whether the mutation in TMEM43 has an impact on its localisation, we performed IF staining on fixed larvae and paraffin sections of adult hearts. In TMEM43-WT and -p.P111L, the TMEM43-eGFP fusion protein localised properly at the nuclear envelope and the endoplasmic reticulum, whereas TMEM43-p.S358L displayed strikingly a delocalization in the cytoplasm and a reduced overall expression. Assessment of the heart morphology at 5 months of age showed that TMEM43-p.S358L ventricles of dissected hearts remain significantly smaller compared to controls as indicated by a reduced ventricular surface area/body length ratio. On ultrastructural level TMEM43-p.S358L ventricular tissue displayed an elevated proportion of nuclei that exhibit expanded perinuclear space and bulging of the outer nuclear membrane.

**Conclusion:** Our results demonstrate that intact TMEM43 seems essential for nuclear morphology and proper cardiac development in transgenic zebrafish. Further examinations will focus on pathways involved in cardiomyocyte growth and proliferation.

#### A 3D model for myocardial infarction in living myocardial slices

N Abbas<sup>1</sup>; F Waleczek<sup>1</sup>; J Fiedler<sup>1</sup>; F Perbellini<sup>1</sup>; T Thum<sup>1</sup>; <sup>1</sup>Hannover Medical School, The Institute of Molecular and Translational Therapeutic Strategies (IMTTS), Hannover, Germany;

**Funding Acknowledgements:** The Institute of Molecular and Translational Therapeutic Strategies (IMTTS)

**Introduction:** Cryoinjury has been recently used as an alternative approach to mimic myocardial infarction in various in vivo studies. This model, often performed in rodents or zebrafish, was shown to be representative for human infarcts encountered in clinical practice. Here, we performed cryoinjury on rat living myocardial slices, which are ultrathin sections of cardiac tissue that maintain the native multicellularity, architecture, and structure of the heart. This in vitro 3D model preserves tissue viability in the absence of coronary perfusion due to free diffusion of oxygen and nutrients into its innermost cells, preventing ischaemic damage and allowing for chronic culture.

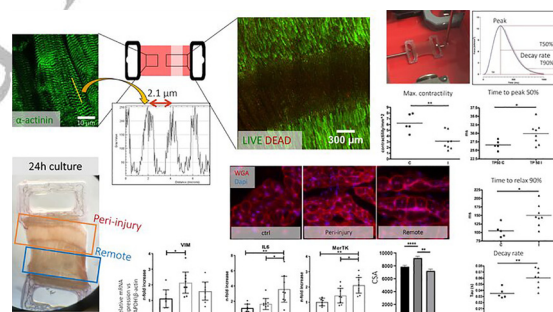
**Purpose:** The aim of this study is to establish in vitro model of myocardial infarction in living myocardial slices using cryoinjury.

**Methods:** Living myocardial slices were generated from rat left ventricular tissue and were subjected to cryoinjury to damage 30% of their length. Cryoinjured slices, along with control slices, were cultured while electromechanically stimulated and mechanically stretched to achieve a sarcomere length of 2.1µm. Force measurements of

freshly prepared slices and cultured slices for 24 and 48 h were performed. Histological studies were done to assess tissue viability, fibrosis markers and cardiomyocyte cross-sectional area. Eventually, slices were cut into two parts: peri-injury (including the cryoinjury with 1mm margins of neighbouring tissue) and remote regions. Both regions were then analyzed for cardiac remodeling marker genes applying real-time PCR.

**Results:** Cell viability assessment using live/dead cell staining demonstrated complete death of cells in the cryoinjured area of myocardial slices. Measurement of contractile force of cryoinjured slices after 24 h in culture revealed reduced maximal contractility and slower kinetics, including time to peak, time to relax and decay rate compared to control slices, indicating that contractile function of myocardial slices deteriorated significantly following cryoinjury. Gene expression analysis highlighted an increase in fibroblast gene activation in the remote region, as well as an increased expression of inflammation markers in the peri-injury region of myocardial slices compared to control. Quantification of cardiomyocyte cross-sectional area demonstrated hypertrophy of cardiomyocytes in the remote region of cryoinjured slices compared to both the peri-injury area and the control slices.

**Conclusions:** Based on contractile, structural and selective transcriptional analysis, we here report a reproducible model of myocardial infarction in living myocardial slices. This 3D model could be utilized for investigating various aspects of cardiac biology, such as electrophysiology, biochemistry and molecular biology, in addition to high applicability in novel drug discovery and regenerative medicine.



Cryoinjury model of MI

#### Metabolic adaptations to dysfunctional mitochondria in Barth Syndrome cardiomyopathy

J Jan Dudek<sup>1</sup>; IK Kutschka<sup>1</sup>; EB Bertero<sup>1</sup>; CW Wasmus<sup>1</sup>; ME Erk<sup>1</sup>; BA Arslan<sup>1</sup>; WS Schmitz<sup>1</sup>; PR Rehling<sup>2</sup>; KG Guan<sup>3</sup>; TH Higuchi<sup>1</sup>; CM Maack<sup>1</sup>; <sup>1</sup>University Hospital Wuerzburg, Wuerzburg, Germany; <sup>2</sup>University Hospital, Göttingen, Germany; <sup>3</sup>University Hospital Dresden, Dresden, Germany;

**Funding Acknowledgements:** The work in the laboratory of the authors is supported by the Deutsche Forschungsgemeinschaft (DFG; DU1839/2-1), the Bundesministerium für Bildung und Forschung (BMBF) and the Barth Syndrome Foundation

As one of the most energy consuming organs in the human body, the heart strongly depends on mitochondrial oxidative phosphorylation to cover its large energy demand. The largest contributor to energy metabolism is the  $\beta$ -oxidation of fatty acids. The compartmentalization of mitochondria by two membranes structurally organize the enzymes of  $\beta$ -oxidation, Krebs cycle and the respiratory chain. The essential functions of the inner membrane critically depends on the hallmark phospholipid cardiolipin (CL). Inherited defects in the biogenesis of CL causes Barth Syndrome (BTHS), which is associated with mitochondrial dysfunction in respiration and the Krebs cycle and cardiomyopathy. CL deficiency not only affects energy conversion but also also abrogates redox homeostasis, another essential function of the mitochondria. Increased consumption of reduction equivalents under conditions of elevated workload, must be compensated by an increase in mitochondrial metabolism. Calcium signals ensure the energetic coupling of mitochondrial and cytosolic metabolism. In BTHS, this coupling is disrupted by a defect in the mitochondrial calcium uniporter (MCU), which transmits calcium emitted from the ryanodine receptor into the mitochondrial matrix.

Using a mouse model for BTHS and patient iPSC derived cardiomyocytes, we show here, that defects in energy and redox homeostasis causes significant changes in cardiac metabolism. Using in vivo PET-CT imaging, we find evidence for an extensive metabolic remodeling, including a considerable reduction in fatty acid oxidation and an increase in glucose metabolism in Barth syndrome. The change in metabolism precedes changes in cardiac function in the mouse model. Transcriptome analyses of the BTHS heart muscle revealed the upregulation of a stress-induced retrograde signaling pathway. Independent of the change in carbohydrate metabolism,

this pathway induces a unique compensatory transformation of metabolism. We describe changes in folate metabolism and alterations in the glutamate metabolism and glutathione biosynthesis, which serve to compensate the defects in mitochondrial energy and redox homeostasis. Targeted interventions in the cell metabolism will enable new strategies for therapeutic intervention in cardiomyopathies with mitochondrial dysfunctions.

#### miR-199a is differentially regulated during physiological and pathological cardiac hypertrophy

L Dumas<sup>1</sup>; V Joris<sup>1</sup>; T Metzinger<sup>1</sup>; D Marchand<sup>1</sup>; H Esfahani<sup>1</sup>; S Kurbanova<sup>1</sup>; L Maistriaux<sup>2</sup>; E Bastien<sup>1</sup>; Ep Daskalopoulos<sup>3</sup>; S Horman<sup>3</sup>; C Dessy<sup>1</sup>; <sup>1</sup>Université Catholique de Louvain, Pole of Pharmacology and Therapeutics (FATH), Experimental and Clinical Research Institute (IREC), Brussels, Belgium; <sup>2</sup>Université Catholique de Louvain, Pole of Morphology (MORF), Experimental and Clinical Research Institute (IREC), Brussels, Belgium; <sup>3</sup>Université Catholique de Louvain, Pole of Cardiovascular Research (CARD), Experimental and Clinical Research Institute (IREC), Brussels, Belgium;

**Funding Acknowledgements:** ARC

**Introduction:** Among potential molecular mechanisms supporting cardiovascular homeostasis, miRNAs (miRs) represent interesting candidates. Our previous work has highlighted a role for miR-199a family members as key regulators of endothelial (dys)function, work from others showing also a dysregulation of the same miRs in cardiomyocytes in the context of pathological cardiac hypertrophy.

**Purpose:** The working hypothesis supporting this work is that alterations in endothelial cell and/or cardiomyocyte phenotypes could be driven by changes in miR-199a abundance, accounting for cardiac and vascular adaptations to exercise. Comparisons with a pathological model of cardiac hypertrophy (induced by transaortic constriction (TAC)) were performed.

**Methods:** Five weeks old male C57Bl6/J mice were given access to voluntary wheel running. After 22 weeks, contractile profile and endothelial function were evaluated ex vivo. A second model consists in a TAC surgery lasting 9 weeks to induced a pathological cardiac hypertrophy. Heart, vessels and plasma were processed for miR profiling and/or protein expression analyses.

**Results:** Moderate exercise induced a significant cardiac remodeling with improved or unaltered cardiac function measured by echo during the 22 weeks protocol. This correlated with an improvement of basal endothelial function attested by NO-dependent repression of contractile tone in arteries of active mice. A down-regulation of miR-199a-3p and miR-199a-5p expression was observed in the heart of running mice, together with increased expression of its direct targets Sirt1 and PGC1 $\alpha$ . miR-199a-5p was also down-regulated in vessels of active mice and this correlated with an up-regulation of endothelial function measured through eNOS and Akt activation. In comparison, TAC mice presented a systematic upregulation of miR-199a-3p/5p expression in cardiac and vascular tissues that correlated with the deleterious remodelling and dysregulated endothelial function. Interestingly, the well-known nuclear factor Twist1, responsible of miR-199a family members expression, was modulated in both models.

**Conclusion:** Our results demonstrate that moderate exercise positively regulates cardiac and endothelial functions potentially through a modulation of miR-199a expression. On the contrary, pathological cardiac hypertrophy is correlated with an increased of miR-199a expression in both cardiac and vascular tissue. miR-199a family should be added to the list of miR modulated by exercise in the cardiovascular system and appears to be at the crossroad between physiology and pathology.

#### CRISPR/dCas9VPR mediated gene activity modulation in mouse and human cardiomyocytes for Krueppel like factor 15 re-activation in cardiac remodeling

E Schoger<sup>1</sup>; C Noack<sup>1</sup>; LM Iyer<sup>2</sup>; L Cyganek<sup>1</sup>; WH Zimmermann<sup>1</sup>; LC Zelarayan<sup>1</sup>; <sup>1</sup>University Medical Center of Göttingen (UMG), Göttingen, Germany; <sup>2</sup>Max Delbrück Center for Molecular Medicine, Berlin, Germany;

**Funding Acknowledgements:** SFB1002-C07, DZHK

**Background:** Cardiac remodeling is accompanied by activation of fetal genes resulting in heart failure. Aberrant activation of WNT/CTNNB1 signaling characterizes heart failure development. This activation triggers chromatin remodeling and fetal gene expression with adverse effects on myocardial performance. We previously identified Krueppel-like factor 15 (KLF15) as a cardiomyocyte-specific inhibitor of WNT/CTNNB1 signaling. Importantly, expression of KLF15 is necessary to maintain mouse and human cardiac function and its expression is reduced in the hypertrophic mouse and in failing human hearts.

**Purpose:** We hypothesize that normalization of KLF15 expression reduces cardiomyocyte hypertrophy and myocardial dysfunction by restoring inhibition of WNT/CTNNB1 signaling. However, gene re-activation to physiologically relevant levels remains challenging. Therefore, we aimed to develop transcriptome engineering tools to restore cardiac homeostasis.

**Methods:** We used CRISPR/Cas9 transcriptional modulation based on enzymatically inactive Cas9 (dCas9) fused to transcriptional activators (VPR). The dCas9VPR complex is recruited by guide RNAs (gRNAs) to the transcriptional start site of genes (CRISPRa) in both, mouse cardiomyocytes and in human induced pluripotent stem cell derived cardiomyocytes (hiPSC-CM) with integrated dCas9VPR at the AAVS1 locus introduced by CRISPR/Cas9 genome editing. We delivered KLF15 gRNAs for gene activation by transducing mouse cardiomyocytes with adeno-associated virus serotype 9 (AAV9) in vivo and by lentiviral transduction of hiPSC-CM.

**Results:** We observed homogenous and long-term expression of dCas9VPR in I) adult mouse cardiomyocytes under the control of Myh6 promoter as well as II) in hiPSC and III) hiPSC-CM driven by CAG promoter. No adverse effects were observed in all conditions and transgene expression was maintained along the course of experiments. KLF15 expression was significantly enhanced by application of both, single and multiple gRNAs, targeted to the 5' upstream transcriptional start site region of KLF15 in CRISPRa hiPSC-CM (n=3-9 experiments, 2 different CRISPRa clones). We found titratability of gene activation by single and multiple gRNAs (1.8 fold change for single and 2.6 fold change for triple gRNA compared to non-targeted gRNAs and control clone). We further used an improved genetically engineered dCas9VPR expression resulting in enhanced KLF15 activation of up to 5.5 fold (n=2 experiments, 2 independent CRISPRa clones).

**Conclusion:** We showed feasibility to modulate gene expression by CRISPR/dCas9VPR in adult mouse and human cardiomyocytes. The titratability of expression levels based on gRNA selection as well as dCas9VPR levels allows for precise gene activity modulation to physiologically relevant expression levels not achievable by classical overexpression approaches. These tools allow us to validate novel therapeutic targets, such as KLF15, to prevent heart failure progression.

## Basic Science – Cardiac Diseases

#### Vitamin D binding protein as a potential biomarker for heart failure in myocarditis: translational animal model reveals mechanism

K Katelyn Bruno<sup>1</sup>; EA Douglass<sup>1</sup>; A Jain<sup>1</sup>; AR Hill<sup>1</sup>; GR Salomon<sup>1</sup>; LT Cooper<sup>1</sup>; A Bucek<sup>1</sup>; MJ Coronado<sup>2</sup>; RR Kew<sup>2</sup>; D Fairweather<sup>1</sup>; <sup>1</sup>Mayo Clinic, Cardiovascular Diseases, Jacksonville, USA; <sup>2</sup>Johns Hopkins University, Environmental Health Sciences, Baltimore, USA;

**Funding Acknowledgements:** None

**Introduction:** An estimated 3.1 million cases of myocarditis/cardiomyopathy were diagnosed in 2017. Myocarditis, inflammation of the myocardium, is a leading cause of sudden death from heart failure in children and young adults worldwide. Patients can progress to dilated cardiomyopathy, heart and heart transplant. Studies have found that Vitamin D binding protein (DBP) could be instrumental in response to tissue injury and activation of the immune response. This chemotaxis activation has been shown to be due to activation of the complement cascade via C5a. The involvement of DBP in disease has never been assessed for myocarditis or other cardiovascular diseases.

**Purpose:** We hypothesize that DBP activates the immune response by altering the complement cascade in a sex-specific manner leading to increased myocarditis. The overall goal of this study is to examine the role of DBP and complement in patients with myocarditis and determine the mechanism whereby DBP alters cardiac inflammation in a translational animal model of viral myocarditis.

**Methods:** We utilized a translational animal model of viral myocarditis to assess the mechanism whereby DBP could alter disease pathway activation and increase acute myocarditis. We also utilized stored serum samples from myocarditis patients and patient data to assess the relationship between DBP levels in patient serum vs. left ventricular (LV) ejection fraction (EF) by sex and age.

**Results:** We found that DBP was upregulated 45-fold in men with myocarditis compared to women and correlated to %EF in women ( $P=0.0004$ ). Additionally we found that men with myocarditis had significantly higher levels of complement C3, C4b, C8 ( $P<0.0001$ ) in their sera than women with disease, suggesting sex differences in DBP and complement influence cardiac inflammation. We found that DBP exacerbates myocarditis using DBP deficient (DBP<sup>-/-</sup>) mice in our animal model of CVB3 myocarditis in both female ( $P=0.009$ ) and male mice ( $P=0.003$ ). Increased disease was attributed to shifts in cytokines; IL-17 ( $P=0.0004$ ) in female mice and IFN $\gamma$  ( $P=0.04$ ) and IL-1b ( $P=0.04$ ) in male mice and increased activation of the complement cascade; C5a (females  $P=0.03$ , males  $P=0.02$ ), CR1 (females  $P=0.04$ ), C3 (females  $P=0.008$ , males  $P=0.04$ ), C3aR1 (males  $P=0.02$ ), C4b (males  $P=0.03$ ), and C5aR1 (males  $P=0.03$ ), in a sex specific manner. We also found in our myocarditis mouse model that sex differences in complement C3 and CR1 may increase susceptibility to myocarditis in males.

**Conclusion:** Our translational animal model of viral myocarditis has revealed that DBP can increase inflammation, myocarditis, by upregulating the complement cascade. We found that having a mechanistic understanding of circulating DBP in patients and mice could be used to predict disease severity in patients with myocarditis and potentially other forms of heart failure.

## Tenascin C promotes cardiac fibrosis, inflammation and endothelial dysfunction in a mouse model of diabetes

A Kiss<sup>1</sup>; ZS Arnold<sup>1</sup>; PL Szabo<sup>1</sup>; E Acar<sup>1</sup>; I Aykac<sup>1</sup>; S Watzinger<sup>1</sup>; F Balogh<sup>2</sup>; A Josvai<sup>3</sup>; M Szekeres<sup>2</sup>; GY Nadasy<sup>2</sup>; BK Podesser<sup>1</sup>; <sup>1</sup>Medical University of Vienna, Center for Biomedical Research, Vienna, Austria; <sup>2</sup>Semmelweis University, Department of Physiology, Budapest, Hungary; <sup>3</sup>Department of Neurosurgery, Medical Centre, Hungarian Defence Forces, Budapest, Budapest, Hungary;

**Funding Acknowledgements:** Stiftung Aktion Österreich-Ungarn

**Background:** Cardiovascular dysfunction in diabetes is characterized by the excessive fibrosis and endothelial dysfunction. More recently, Tenascin-C (TN-C) upregulation in the myocardium and serum predicts worse outcome in diabetic and heart failure patients. However, the causative role of TN-C in fibrosis and vascular dysfunction remains elusive in diabetes.

**Methods:** AJ and TNC-KO adult male mice were repeatedly injected with streptozotocin. Cardiac function was assessed by echocardiography at baseline and at 18-20 weeks follow-up. Vascular endothelial function was performed by using wire myography in isolated abdominal aorta segments. Cardiac fibrosis was assessed by histochemistry. In addition, the hemodynamic effects of recombinant human TN-C (rhTN-C) on isolated rat hearts were evaluated on erythrocyte-perfused, isolated working heart system. Furthermore, human ventricular cardiac fibroblasts (HCF) were cultured, then starved and treated with 1) TGF- $\beta$ ; 2) rhTN-C (10  $\mu$ g/ml) and TLR4 inhibitor in combination with TN-C and subsequently mRNA expression of  $\alpha$ -SMA, TN-C, Col-1, Col-3, LOX1-4 and ACE1 were assessed by RT-qPCR. In addition, human umbilical vein endothelial cells (HUVEC) were treated either with rhTN-C (10  $\mu$ g/ml) or combination with TLR-4 inhibitor (TAK-242, 50nM) and analysed the expression of NADPH oxidase 1 and 4 (NOX1, NOX4), and interleukin-6 (IL-6).

**Results:** Blood glucose levels of AJ and TNC-KO animals did not, however lack of TN-C was accompanied by preserved ejection fraction ( $P < 0.05$ ) and endothelium-dependent relaxation in compared to diabetic AJ mice, respectively (at 18 weeks,  $P < 0.05$  and  $P < 0.001$ ). Histology revealed less cardiac and perivascular fibrosis in TNC-KO diabetic animals than in the AJ diabetic group ( $P < 0.01$ , respectively). In addition, cumulative dosage of rhTN-C (80 ng/ml) resulted a significant reduction in cardiac output ( $P < 0.01$ ) and LV systolic pressure ( $P < 0.05$ ) in association with a massive upregulation of TNF- $\alpha$  and IL-1 $\beta$  in isolated rat hearts. TGF- $\beta$  treatment resulted in TN-C upregulation of expression in HCF ( $P < 0.01$ ). Notably, HCF were exposed to rhTN-C promoted both  $\alpha$ -SMA and Col 1 and 3 as well as LOX 1-4 mRNA expression, respectively ( $P < 0.05$ ). In addition, HUVEC incubated with rhTN-C showed increased expression of IL-6 and oxidative stress-related markers (NOX4) and TLR-4 inhibitor pre-treatment markedly reversed these changes.

**Conclusions:** These findings uncover a novel mechanism that TN-C contributes to cardiovascular dysfunction in diabetes. TN-C created an intracellular environment that facilitated fibrosis and oxidative stress, which, in turn, resulting in cardiomyocyte and endothelial cell dysfunction. Thus, TN-C may be a critical mediator of the progression of cardiovascular dysfunctions in diabetes as well as a potential target for future therapy.

## Characterization of molecular mechanisms underlying dilated cardiomyopathy with ataxia (DCMA) using pluripotent stem cell (iPSC)-derived cardiomyocytes

A Janz<sup>1</sup>; A Cirnu<sup>1</sup>; M Leskien<sup>1</sup>; A Seewald<sup>1</sup>; Y Ueda<sup>2</sup>; M Regensburger<sup>1</sup>; M Kohlhaas<sup>3</sup>; p Woersdoerfer<sup>2</sup>; N Wagner<sup>2</sup>; E Klopocki<sup>4</sup>; T Higuchi<sup>5</sup>; H Duff<sup>6</sup>; C Maack<sup>3</sup>; S Erguen<sup>2</sup>; B Gerull<sup>1</sup>; <sup>1</sup>Comprehensive Heart Failure Center, Cardiovascular Genetics, Wuerzburg, Germany; <sup>2</sup>Medical faculty of the University of Wuerzburg, Institute of Anatomy and Cell Biology, Wuerzburg, Germany; <sup>3</sup>Comprehensive Heart Failure Center (CHFC), Translational Research, Wuerzburg, Germany; <sup>4</sup>University of Wuerzburg, Institute of Human Genetics, Wuerzburg, Germany; <sup>5</sup>Comprehensive Heart Failure Center (CHFC), Nuclear Medicine, Wuerzburg, Germany; <sup>6</sup>Libin Cardiovascular Institute Of Alberta, Cardiac Sciences, Calgary, Canada;

**Funding Acknowledgements:** 01EO1504 Federal Ministry of Education and Research, Germany (BMBF)

**Background:** Dilated cardiomyopathy with ataxia (DCMA) is an autosomal recessive disorder characterized by life threatening early onset cardiomyopathy associated with a metabolic syndrome. DCMA is caused by mutations in the DNAJC19 encoding an inner mitochondrial membrane (IMM) protein with a presumed function in mitochondrial biogenesis and cardiolipin remodeling via direct interaction with prohibitin 2 (PHB2).

**Methods and Results:** A novel human iPSC-based in vitro platform was generated to investigate DCMA by reprogramming of two patient-derived lines of siblings with discordant cardiac phenotypes and a CRISPR/Cas9-edited isogenic Mutant (DNAJC19tv). Mutant and control iPSC-derived cardiomyocytes (iPSC-CMs) were characterized at a mature stage. The mutation was predicted to cause a loss of the DnaJ interaction domain, which was confirmed by loss of full-length DNAJC19 protein in all mutant cell lines. Subcellular investigation of DNAJC19 demonstrated

a nuclear restriction in mutant iPSC-CMs. The loss of DNAJC19 co-localization with mitochondrial structures was accompanied by enhanced fragmentation, an overall reduction of mitochondria mass and smaller cardiomyocytes. Ultrastructural analysis yielded decreased mitochondria sizes and abnormal cristae providing a link to defects in mitochondrial biogenesis and cardiolipin remodeling. Examination of mitochondrial function revealed an overall higher oxygen consumption rate (OCR) in all mutant iPSC-CMs compared to controls indicating a higher electron transport chain activity. Double radioactive tracer uptakes (18F-FDG, 125I-BMIPP) showed decreased fatty acid uptake that was in one patient cell line accompanied by increased glucose uptake. IonOptix measurements (Indo-1 AM) were performed to get insights on Ca<sup>2+</sup> kinetics, contractility and arrhythmic potential on >120 days mattress-matured iPSC-CMs. Significantly increased beating frequencies, elevated diastolic Ca<sup>2+</sup> concentrations and a shared trend towards reduced sarcomere shortenings were observed in all mutant cell lines basally and upon isoproterenol stimulation. Extended speed of recovery was seen in all mutant iPSC-CMs but most striking the male patient cells additionally showed significantly prolonged relaxation times. Investigations of Ca<sup>2+</sup> transient shapes unraveled enhanced arrhythmic features in mutant cells, comprised by both the occurrence of DADs/EADs and fibrillation-like events with discordant preferences.

**Conclusion:** We suggest that loss of full-length DNAJC19 impedes PHB2-complex stabilization within the IMM, thus hindering PHB-rings from building IMM-specific phospholipid clusters. These clusters are essential to enable normal cardiolipin remodeling during cristae morphogenesis. Disturbed cristae and mitochondrial function refer to an essential role of DNAJC19 in mitochondrial morphogenesis and biogenesis. Moreover, excess OCRs, altered substrate utilization and abnormal Ca<sup>2+</sup> kinetics enables insights into the pathogenesis of DCMA.

## HDAC inhibition regulates cardiac function by increasing myofilament calcium sensitivity and decreasing diastolic tension

DM Eaton<sup>1</sup>; TG Martin<sup>2</sup>; M Kasa<sup>3</sup>; N Djalinac<sup>3</sup>; JP Johnson<sup>1</sup>; E Kolesnik<sup>3</sup>; S Ljubojevic-Holzer<sup>3</sup>; D Von Lewinski<sup>3</sup>; H Maechler<sup>4</sup>; A Zirkik<sup>3</sup>; JA Kirk<sup>2</sup>; SR Houser<sup>1</sup>; PP Rainer<sup>3</sup>; M Wallner<sup>3</sup>; <sup>1</sup>Temple University School of Medicine, Cardiovascular Research Center, Philadelphia, USA; <sup>2</sup>Loyola University Chicago Stritch School of Medicine, Department of Cell and Molecular Physiology, Chicago, USA; <sup>3</sup>Medical University of Graz, Department of Cardiology, Graz, Austria; <sup>4</sup>Medical University of Graz, Department of Cardiothoracic Surgery, Graz, Austria;

**Funding Acknowledgements:** European Research Area Network on Cardiovascular Diseases (ERA-CVD)/Austrian Society of Cardiology

**Background/Introduction:** Heart Failure with preserved Ejection Fraction (HFpEF) accounts for approximately 50% of all HF diagnoses with no proven effective therapies. We established a large animal model of slow progressive pressure overload that recapitulates key clinical features of HFpEF. We then tested the effects of the pan-HDAC inhibitor suberanilohydroxamic acid (SAHA) in the model and found that SAHA reversed and prevented the development of diastolic, systolic, and pulmonary dysfunction.

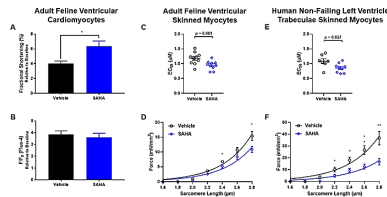
**Purpose:** Evaluate the effects of SAHA at the level of cardiomyocyte and contractile protein function to understand how it modulates cardiac function in parallel studies using cardiac tissue from humans and large mammals with similar physiological features (i.e. long action potential, similar myosin heavy chain isoform).

**Methods:** Adult feline ventricular cardiomyocytes (AFVM) were isolated from male domestic short hair cats and treated with 2.5  $\mu$ M SAHA or vehicle (DMSO) for 90 min, then incubated with a calcium (Ca<sup>2+</sup>) indicator (Fluo-4AM) and electrically stimulated (0.5Hz) to record Ca<sup>2+</sup> transients and contractions. Skinned myocytes were isolated from treated AFVM and functional experiments were performed to assess myofilament Ca<sup>2+</sup> sensitivity and passive stiffness. The effects of SAHA on human cardiac tissue was assessed using left ventricle (LV) trabeculae isolated from non-failing donor hearts treated with 10  $\mu$ M SAHA or vehicle for 120 min while being electrically stimulated (1Hz). Developed force and relaxation parameters were recorded. Skinned myocytes were then isolated for calcium sensitivity and passive stiffness experiments.

**Results:** SAHA treated AFVM had a significant increase in contractility (fractional shortening) and improved relaxation kinetics (time to 50% baseline, return velocity), but no difference in peak Ca<sup>2+</sup> transients (Figure A, B). These findings are indicative of an increase in myofilament Ca<sup>2+</sup> sensitivity. Skinned myocytes, used to assess myofilament function, were isolated from treated AFVMs. There was a significant increase in myofilament Ca<sup>2+</sup> sensitivity and significant decrease in passive stiffness with SAHA (Figure C, D). Extending these findings to human cardiac tissue, SAHA treated trabeculae isolated from non-failing hearts had decreased diastolic tension and increased developed force, with a similar systolic peak force. Skinned myocytes isolated from these trabeculae had a similar response to AFVMs, with an increase in myofilament Ca<sup>2+</sup> sensitivity and decrease in passive stiffness (Figure E, F).

**Conclusions:** These findings suggest that SAHA has an important role in the direct control of cardiac function at the level of the cardiomyocyte and myofilament in human and feline myocardium by increasing myofilament calcium sensitivity and reducing diastolic tension. These changes are consistent with functional data

observed in human trabeculae and in-vivo hemodynamics in a feline model with features of HFpEF.



Cardiomyocyte and myofilament function

### Mechanistic insights of the p.L13R mutation in the inner nuclear membrane protein Lemd2 leading to cardiomyopathy associated with arrhythmias

R Ruping Chen<sup>1</sup>; G Gruener<sup>1</sup>; Ap Arias-Loza<sup>1</sup>; M Kohlhaas<sup>1</sup>; A Nickel<sup>1</sup>; T Williams<sup>1</sup>; C Maack<sup>1</sup>; B Gerull<sup>1</sup>; <sup>1</sup>Comprehensive Heart Failure Center (CHFC), Würzburg, Germany;

**Funding Acknowledgements:** 01EO1504 Federal Ministry of Education and Research, Germany (BMBF)

**Background and Purpose:** Nuclear envelope proteins play important roles in the pathogenesis of hereditary cardiomyopathies. We recently discovered a new form of arrhythmic cardiomyopathy caused by a homozygous mutation (p.L13R) in the inner nuclear membrane (NM) protein LEMD2. We generated a knock-in (KI) mouse model carrying Lemd2 p.L13R mutation to unravel the molecular mechanisms underlying the human mutation.

**Methods and Results:** Homozygous KI mice were viable and phenotypically characterized at 6 months (6m) and 9 months (9m) old ages. Cardiac function assessed by echocardiography revealed a severe form of cardiomyopathy with left ventricular (LV) systolic dysfunction, increased LV end-systolic diameter and decreased LV wall thicknesses in 9m KI mice. At the same age surface electrocardiograms (ECGs) displayed pronounced arrhythmias. Further ECG analysis demonstrated prolonged PR, QRS and corrected QT intervals indicating conduction and repolarization abnormalities.

Histology staining revealed mild cardiac fibrosis in 6m KI hearts with subsequent severe fibrosis at the age of 9 months. Interestingly, cardiomyocyte hypertrophy measured as an enlarged cross-sectional area indicated an early hallmark already at 3m of age which further increased until 9m of age. We hypothesized that cellular hypertrophy might be a result from reduced proliferation capacity at the postnatal stage and confirmed a reduced cardiomyocyte proliferation and lower cardiomyocyte cell counts in postnatal day 5 old KI mice. To study the mechanisms towards premature cellular senescence, we scrutinized if the p53/p21 pathway might play a role in the disease and detected higher p53 protein levels in KI hearts. Senescence-associated secretory phenotype related genes were also up-regulated in addition to increased DNA damage (YH2AX) in 9m old KI hearts.

As LEMD2 plays a role in heterochromatin remodeling, we performed TEM which showed invaginations of the nuclear membrane (NM), detached heterochromatin and an expanded distance between the outer and inner NM. In addition, we detected a compromised interaction between mutant LEMD2 and the Barrier-to-autointegration factor (BAF) which is an important component of chromatin remodeling complex. Further investigations will unravel if the process of repair following NM ruptures requiring an interplay of BAF, LEMD2 and ESCRT-III. Potentially unrepaired ruptures compromise retention of DNA repair factors and favor sustained damage.

**Conclusion:** We showed that the Lemd2 p.L13R mutation in mice recapitulates the human phenotype leading to cardiomyopathy with cardiomyocyte hypertrophy, fibrosis and severe arrhythmias. The mutation leads to a compromised postnatal proliferation capacity, induces increased DNA damage and causes premature cellular senescence. We propose that a disturbed interaction between LEMD2 and BAF and subsequent impaired NM repair may play a role in the pathogenesis of the disease.

### Mitochondrial dysfunction in tachycardiomyopathy

M Paulus<sup>1</sup>; K Renner<sup>2</sup>; S Pabel<sup>1</sup>; E Zuegner<sup>3</sup>; C Magnes<sup>3</sup>; G Pietrzyk<sup>1</sup>; D Riedl<sup>1</sup>; A Luchner<sup>4</sup>; C Birner<sup>5</sup>; S Wagner<sup>1</sup>; LS Maier<sup>1</sup>; K Streckfuss-Boemeke<sup>6</sup>; ST Sossalla<sup>1</sup>; A Dietl<sup>1</sup>; <sup>1</sup>University hospital Regensburg, Department of Internal Medicine II, Regensburg, Germany; <sup>2</sup>University hospital Regensburg, Department of Internal Medicine III, Regensburg, Germany; <sup>3</sup>Joanneum Research Health, Institute for Biomedicine and Health Sciences, Graz, Austria; <sup>4</sup>Krankenhaus der Barmherzigen Brüder, Clinic for Cardiology, Regensburg, Germany; <sup>5</sup>Klinikum St. Marien,

Department of Internal Medicine I, Amberg, Germany; <sup>6</sup>University Medical Center of Göttingen (UMG), Clinic for Cardiology and Pneumology, Göttingen, Germany;

**Funding Acknowledgements:** REFORM research grant from the University of Regensburg

**Background:** Clinical significance of tachycardiomyopathy increased with trials on catheter ablation therapy. Human endomyocardial biopsies show alterations of mitochondrial architecture.

**Purpose:** To investigate mitochondrial function in the pathophysiology of tachycardiomyopathy.

**Methods:** Pacemaker implantation was performed in 14 rabbits. 7 underwent tachypacing with 380bpm (TCM), while in 7 rabbits the pacemaker remained inactive (SHAM). Left ventricular tissue was subjected to histologic examination, transmission electron microscopy, mass-spectrometry-based metabolomic profiling (LC-HRMS), and targeted transcriptomics of 168 genes of mitochondrial metabolism. Results from the animal model were evaluated for their translational potential using a human-based model. Induced pluripotent stem cell cardiomyocytes (iPS-CM) of 4 healthy donors underwent electric field stimulation (7 days, 120bpm, TACH vs. 60bpm, CTRL) in a paired design. Fluorometry (Amplex Red) and flow cytometry (MitoSOX Red, MitoTracker Green) were performed. For functional evaluation, high-resolution respirometry was established in intact tissue and cells, measuring oxidative capacity while avoiding artefacts caused by mitochondria isolation.

**Results:** TCM animals showed left ventricular dilatation and systolic dysfunction ( $\Delta$ LVEDD  $+5.3 \pm 0.2$ mm;  $\Delta$ FS  $-19 \pm 8\%$ ; TCM-SHAM;  $P < 0.001$ ). Histology revealed cardiomyocyte hypertrophy (cross-sectional area  $519 \pm 32$  vs.  $413 \pm 21 \mu\text{m}^2$ ,  $P < 0.01$ ) without fibrosis (hydroxyproline content,  $P = 0.52$ ). Findings in electron microscopy included mitochondrial pleomorphism and increased cristae density in TCM animals, suggesting a disturbance of mitochondrial membrane organization. Oxidative phosphorylation capacity in TCM animals was decreased ( $133 \pm 13$  vs.  $170 \pm 16$  pmol  $\cdot$  O<sub>2</sub>  $\cdot$  s<sup>-1</sup>  $\cdot$  mg<sup>-1</sup> tissue,  $P < 0.05$ ), which was also observed in iPS-CM after tachypacing ( $995 \pm 738$  vs.  $1838 \pm 901$  pmolO<sub>2</sub>  $\cdot$  s<sup>-1</sup>  $\cdot$  IU<sup>-1</sup> citrate synthase activity, TACH vs. CTRL,  $P < 0.01$ ). Principal component analysis of LC-HRMS-based metabolomics revealed clustering of SHAM and TCM in two distinct groups, underlying profound alterations of metabolism in TCM. As mitochondrial content in iPS-CM remained unchanged after tachypacing (MitoTracker Green-FACS,  $P = 0.57$ ), these findings hinted towards mitochondrial dysfunction. Mitochondrial transcriptomics were characterized by altered expression of components of ROS homeostasis, including downregulation of antioxidative enzymes (e.g. glutathione peroxidase 3, fold change (FC) TCM/SHAM 0.5,  $P < 0.05$ ) and upregulation of the ROS-producing enzyme NOX4 (FC 2.1,  $P < 0.05$ ). On a functional level, both H<sub>2</sub>O<sub>2</sub> and mitochondrial superoxide emission were increased in iPS-CM after tachypacing (H<sub>2</sub>O<sub>2</sub> Amplex Red  $1.65 \pm 0.20$  vs.  $1.03 \pm 0.11 \mu\text{M}/106$  cells; MitoSOX-FACS MFU  $439 \pm 166$  vs.  $279 \pm 99$ , TACH vs. CTRL,  $P < 0.05$ ).

**Conclusion:** Tachycardiomyopathy implicates a disturbance of two mitochondrial key functions: oxidate phosphorylation capacity is reduced, while ROS emission increases.

### Role and regulation of unconventional motor proteins myosin 5a and 5b in the heart

M Heimerl<sup>1</sup>; M Ricke-Hoch<sup>1</sup>; S Erschow<sup>1</sup>; S Pietzsch<sup>1</sup>; M Scherr<sup>2</sup>; D Hilfinger-Kleiner<sup>1</sup>; <sup>1</sup>Hannover Medical School, Department of Cardiology and Angiology, Hannover, Germany; <sup>2</sup>Hannover Medical School, Department of Hematology, Hemostasis, Oncology and Stem Cell Transplantation, Hannover, Germany;

**Funding Acknowledgements:** KFO311

**Introduction:** The myosin (Myo) superfamily consists of motor proteins involved in cell motility, contraction and intracellular transport. Myo5a and Myo5b perform directional movement along cytoplasmic actin filaments, thereby acting as cargo transporters of cell organelles, vesicles, receptors and signalling molecules.

**Purpose:** We aim to analyse the regulation and function of Myo5a and 5b in cardiomyocytes and in the adult mouse heart.

**Methods and Results:** mRNA expression analysis revealed a developmental specific regulation of Myo5a and 5b expression in cardiomyocytes with Myo5a as the major isoform in embryonic/fetal and Myo5b as the predominant isoform in adult cardiomyocytes. Myo5b expression is reduced in human failing hearts and in neonatal rat cardiomyocytes stimulated by proinflammatory cytokines (TNF $\alpha$  and IFN $\gamma$ ). To analyse the role of Myo5b, mice with a cardiomyocyte-specific knockout of Myo5b (Myo5b-KO) were generated. They were born at the expected Mendelian ratio with no indication of morphological abnormalities and normal contractility (FAC) up to the age of 12 weeks (w). However, electrocardiogram recordings (HOLTER analyses) revealed intermittent bundle branch blocks, alterations in the periods between QRS-complexes, supraventricular extra-systoles and atrial fibrillation. Thereafter, male and female Myo5b-KO mice gradually developed a dilated cardiomyopathy (FAC 24w: WT male:  $50 \pm 15\%$  vs. Myo5b-KO male:  $27 \pm 12\%$ ;  $P < 0.0001$ ; n=20-22; WT female:  $52 \pm 12\%$  vs. Myo5b-KO female  $38 \pm 13\%$ ;

$P < 0.001$ ;  $n = 19-21$ ). Development of heart failure was accompanied by inflammation, fibrosis and age-related mortality (all KO mice died at  $34 \pm 3$  w). RNAseq analyses at the age of 12 weeks revealed 796 altered genes ( $p\text{-adj.} < 0.05$ ) and 70 altered pathways (DAVID tool;  $p\text{-adj.} < 0.05$ ) between WT and Myo5b-KO hearts ( $n = 9-10$ ). Among those were alterations in neuroendocrine and metabolic pathways. Further analyses revealed a reduction in GLUT4 expression and insulin-induced glucose uptake to cardiomyocytes in Myo5b-deleted cardiomyocytes. In addition, altered expression of genes involved in the structure and functionality of the sarcomere, i.e. downregulation of TPM1, TNNI3, ACTN2, AbBLIM1, SERCA2 and MYO6 and upregulation of MYBPC3 were observed in Myo5b-KO hearts. First evidence suggests a role for Myo5b in mRNA transport.

**Conclusion:** Our results highlight a differential regulation of Myo5a and 5b during the development of cardiomyocytes with Myo5b being the dominant form in the adult heart. Deletion of Myo5b in cardiomyocytes leads to age-related dilated cardiomyopathy, associated with impaired expression of genes involved in metabolism, neuroendocrine signalling and sarcomere structure and function. First analyses suggest a role for Myo5b in glucose and mRNA transport.

### Mir181a is a novel regulator of aldosterone mineralocorticoid receptor mediated cardiac remodelling

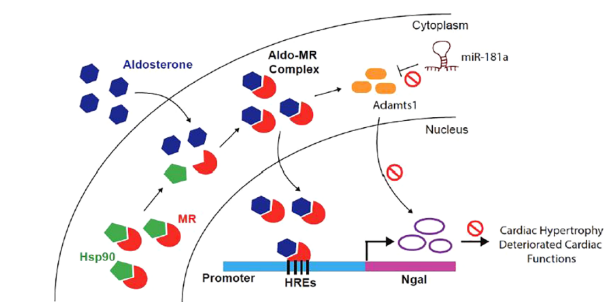
A Garg<sup>1</sup>; A Foinquinos<sup>1</sup>; M Jung<sup>1</sup>; H Janssen-Peters<sup>1</sup>; S Biss<sup>1</sup>; J Bauersachs<sup>1</sup>; SK Gupta<sup>1</sup>; T Thum<sup>1</sup>; <sup>1</sup>Hannover Medical School, Hannover, Germany;

**Funding Acknowledgements:** Deutsche Forschungsgemeinschaft (DFG) DFG TH 903/18-1 \nBA1742/8-1

**Aim:** The aldosterone-mineralocorticoid receptor (Aldo-MR) pathway is activated during cardiac stress, such as hypertension, myocardial infarction (MI), and heart failure. The importance of Aldo and MR in the pathogenesis of cardiac diseases is well established; however, the regulatory mechanisms behind Aldo/MR-induced cardiac remodelling remain uncertain. We here investigated potential miRNA-mediated regulation of the Aldo-MR pathway to improve mechanistic understanding.

**Methods and Results:** High-throughput screening of 2,555 miRNAs using an MR responsive stable cardiomyocyte cell line (MMTV-GFP-HL-1) identified miR-181a as a potential regulator of Aldo-MR pathway. MiR-181a was found to downregulate the expression of Ngai (lipocalin-2), a well-established downstream effector molecule of Aldo-MR. In addition, Aldo-induced cellular hypertrophy decreased significantly upon miR-181a overexpression. Genetic miR-181 knockout in murine MI model led to deteriorated cardiac function, cardiac remodelling, and activation of Aldo-MR pathway while AAV9-mediated miR-181a overexpression improved cardiac function and deactivated Aldo-MR pathway proving a cardio-protective role of miR-181a. Global RNA sequencing of cells under Aldo treatment with/without miR-181a overexpression identified potential miR-181a targets functionally contributing to Aldo-MR pathway. Adamts1, a direct target of miR-181a, was found to be downregulated with miR-181a overexpression and upregulated with inhibition. Similar to miR-181a overexpression, siRNA-mediated inhibition of Adamts1 inhibited Aldo-MR pathway.

**Conclusion:** We here show that miR-181a is a novel regulator of the Aldo-MR pathway regulating the levels of Ngai via direct targeting of Adamts1. This new insight establishes miR-181a as a factor of immense value participating in downstream networks of Aldo-MR pathway. Our in vivo studies further confirmed miR-181a as cardio-protective under MI stress. Thus, miR-181a's involvement in Aldo-MR-mediated cardiac remodelling confers it with tremendous potential to be developed further as a new therapeutic target.



Mir181a regulates Aldo-MR Pathway

### Haematopoietic and cardiac GPR55 synchronize post-myocardial infarction remodelling

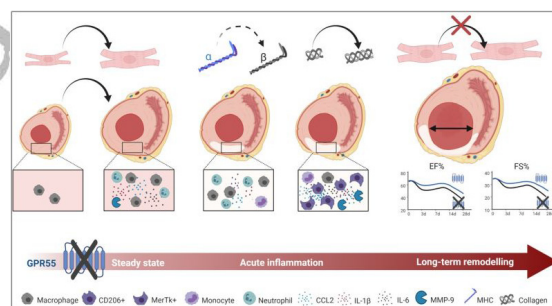
SL Sarah-Lena Puhl<sup>1</sup>; M Hilby<sup>1</sup>; L Keidel<sup>1</sup>; J Schindler<sup>1</sup>; M Hristov<sup>1</sup>; Y Jansen<sup>1</sup>; S Steffens<sup>1</sup>; <sup>1</sup>Ludwig-Maximilians University, Institute for Cardiovascular Prevention (IPEK), Munich, Germany;

**Funding Acknowledgements:** STE-1053/5-1 Deutsche Forschungsgemeinschaft

**Background:** Long-term prognosis after myocardial infarction (MI) is predominantly determined by the extent of ischaemia triggered inflammation and remodelling. Experimental targeting of either the immune- or the endocannabinoid-system revealed promising strategies to improve post MI outcome.

**Purpose:** We aimed at characterizing the role of the cannabinoid-sensitive receptor GPR55 in post MI cardiac inflammation and remodelling.

**Methods:** Cardiac cell-specific GPR55 gene expression was assessed in cardiomyocytes, macrophages, endothelial cells and fibroblasts sorted from adult wild-type (WT) hearts (flow cytometry, qPCR). Global GPR55<sup>-/-</sup> (KO) and WT mice were basally characterized or assigned to MI for 1, 3, 5 or 28 days and subsequently analysed via pro-inflammatory (flow cytometry, qPCR, ELISA) and pro-hypertrophic parameters (gravimetry, histology, echocardiography, qPCR). To elicit the haematopoietic role of GPR55, KO>WT bone marrow chimera were generated, subjected to 3 days MI and characterized regarding cardiac inflammation. WT>WT chimera served as controls.



GPR55 synchronizes post MI remodelling

**Results:** Naïve GPR55<sup>-/-</sup> mice exhibited a volume-overloaded heart, indicated by increased diastolic left ventricular (LV) cavity, volume, heart weight and an immune response resembling the stretch-induced inflammation. After MI, acute LV chemokine expression was attenuated in GPR55<sup>-/-</sup> mice at day 1, yet, potentiated at day 3 and even prolonged until day 5 post MI, despite initial infarct sizes comparable to WT. While having no effect on LV neutrophil or monocyte infiltration, 3 days post MI, global GPR55 knock-out (KO) increased cardiac abundance of macrophages expressing mannose-receptor (CD206) and myeloid-epithelial-reproductive tyrosine kinase (MERTK) - hallmarks of pro-reparative and phagocytic macrophages. This was accompanied by potentiated up-regulation of matrix metalloproteinase (Mmp) 9 and collagens (Col) 1a2 and 1a1 in the infarcted heart. In support of a role for GPR55 in cardiac macrophages, we detected its gene expression in macrophages sorted from WT hearts. All observations 3 days post MI could be mimicked by sole haematopoietic GPR55 depletion in KO>WT bone marrow chimera in comparison to WT>WT controls. Regarding hypertrophy, lack of GPR55 mitigated early MI induced fetal gene re-programming and aggravated features of long-term remodelling such as infarct thinning and LV dilatation culminating in a more severe functional decline post MI.

**Conclusion:** Our study alludes for the first time in vivo toward a contributory role of GPR55 to development of LV volume-overload, synchronization of post MI wound healing and regulation of LV remodelling.

### The glycoprotein Dickkopf-3: a new player for the maintenance of vascular homeostasis

A Albino Carrizo<sup>1</sup>; CL Busceti<sup>2</sup>; P Di Pietro<sup>2</sup>; R Ginerete<sup>2</sup>; M Ciccarelli<sup>1</sup>; S Rubattu<sup>2</sup>; F Nicoletti<sup>2</sup>; C Vecchione<sup>1</sup>; <sup>1</sup>University of Salerno, Baronissi, Italy; <sup>2</sup>Ircs I.N.M. Neuromed, Vascular Pathophysiology, Pozzilli, Italy;

**Funding Acknowledgements:** (Project code: GR-2011-02350132, 2011). This work was supported by the Italian Ministry of Health

Dickkopf-3 (Dkk3) is a secreted glycoprotein known for its proapoptotic and angiogenic activity. We used both mice and rats to unravel a role for Dkk3 in the regulation of blood pressure (BP). Genetic deletion of Dkk3 in mice enhanced systolic BP and impaired endothelium-dependent acetylcholine (ACh)-induced relaxation

of mesenteric arteries. Hypertension occurring in Dkk3<sup>-/-</sup> mice was rescued by lentivirus-encoded Dkk3 expression both in the periphery and within the CNS. Exogenous Dkk3 also rescued ACh-induced vasorelaxation. Endogenous Dkk3 was required for constitutive expression of vascular endothelium growth factor (VEGF), and its BP-lowering effect was mediated by VEGF induction followed by activation of type-2 VEGF receptors, stimulation of the phosphatidylinositol-3-kinase pathway, and Akt-driven phosphorylation of endothelial nitric oxide synthase (eNOS). This novel function of Dkk3 was confirmed in spontaneously hypertensive rats (SHRs), in which central overexpression of Dkk3 lowered BP, whereas Dkk3 silencing amplified the hypertensive phenotype. Interestingly, stroke-prone SHRs (SHRsp rats) feature a severe reduction in Dkk3 levels within the lower brainstem, a brain region that is critically involved in BP regulation. When SHRsp rats are challenged with a hypersodic diet, overexpression of Dkk3 in the CNS counteracts the progression of malignant hypertension and delays the occurrence of stroke.

#### Cardiac pericytes can be pharmacologically redirected towards a smooth muscle phenotype to enhance the revascularisation of the ischemic heart

E Avolio<sup>1</sup>; R Katere<sup>2</sup>; AC Thomas<sup>1</sup>; A Caporali<sup>3</sup>; D Schwenke<sup>2</sup>; M Meloni<sup>3</sup>; M Caputo<sup>1</sup>; p Madeddu<sup>1</sup>; <sup>1</sup>University of Bristol, Bristol Medical School, Bristol, UK; <sup>2</sup>University of Otago, Department of Physiology, HeartOtago, Dunedin, New Zealand; <sup>3</sup>University of Edinburgh, Centre for Cardiovascular Science, Edinburgh, UK;

**Funding Acknowledgements:** RM/17/3/33381 British Heart Foundation (BHF) Centre for Regenerative Medicine Award (II) - "Centre for Vascular Regeneration"

**Background:** Pericytes (PC) are abundant cells that wrap around the whole vasculature of the heart. To date, it is not known if PC contribute to the maturation of new arterioles in the ischemic heart.

**Purpose:** we verified whether cardiac PC differentiate into contractile vascular smooth muscle cells (VSMC) in vitro, and if this potential can be pharmacologically induced to enhance the revascularisation of the heart post ischemia in vivo.

**Methods and Results:** PC were extracted from adult myocardial tissue, expanded in vitro, and characterised for antigenic profile and function. At baseline, PC do not express contractile VSMC antigens  $\alpha$ SMA, CALP, SM22 $\alpha$ , SM-MHC and Smoothelin B. We discovered that the inhibition of MEK1/2 activity and ERK1/2 signalling using the small molecule PD0325901 redirects the PC towards a VSMC phenotype. Contraction, calcium flux and migration assays confirmed that differentiated PC became stationary contractile cells, phenocopying control coronary artery SMC (CASM). We further verified this finding using next-generation RNA-sequencing, which showed that differentiated PC expressed a cluster of contractile VSM transcripts similarly to control CASMC. Moreover, treated PC acquired a unique pro-angiogenic transcriptional profile, upregulating pro-angiogenic genes LEP and PDGFB while downregulating potent angiogenesis inhibitors ANGPT2, TIE1 and SERPINF1. We also verified that human PC acquire contractile VSM markers when injected subcutaneously in mice. We next validated this innovative approach in vivo. Healthy C57BL6/J mice given the drug orally, for two weeks, showed an increase in the small arteriole density along with an improved myocardial perfusion, when compared with mice given vehicle. Last, administration of PD0325901 to mice with myocardial infarction improved left ventricular function and induced an increase in both capillary and arteriole density in the peri-infarct area, when compared with controls given vehicle. Improved revascularisation resulted in reducing infarct expansion in PD0325901-treated mice.

**Conclusion:** We propose a novel therapeutic approach based on MEK inhibition to promote the revascularisation of the infarcted heart reawakening the plasticity of resident PC. This approach could benefit the treatment of patients with coronary artery disease.

#### In vivo proteomics identifies lumican as an inhibitor of angiogenesis in the adult mammalian heart

T Kocijan<sup>1</sup>; O Shevchuk<sup>2</sup>; R Elmergawy<sup>1</sup>; S Vodret<sup>1</sup>; A Colliva<sup>1</sup>; C Kern<sup>3</sup>; A Sickmann<sup>2</sup>; M Myers<sup>1</sup>; S Zacchigna<sup>1</sup>; <sup>1</sup>International Centre for Genetic Engineering and Biotechnology (ICGEB), Trieste, Italy; <sup>2</sup>Leibniz Institute for Analytical Sciences, Dortmund, Germany; <sup>3</sup>Medical University of South Carolina, Charleston, USA;

**Funding Acknowledgements:** AIRC

**Background:** Mammalian heart loses its spontaneous regenerative potential during the first week after birth. One of the major differences between regenerating and non-regenerating hearts is adaptation of extracellular matrix (ECM) to injury. Whereas in regenerating hearts ECM remodelling after injury favours cellular migration and invasion of the injured site, in non-regenerating hearts increased collagen deposition and scarring prevent cardiac regeneration. Angiogenesis is a prerequisite for regeneration and, consistent with its low regenerative capacity, the adult heart does not form new vessels in response to pro-angiogenic stimuli.

**Purpose:** This work aims at profiling the proteome of vascular cells and the surrounding ECM of neonatal and adult heart in vivo to identify proteins controlling cardiac angiogenesis.

**Methods:** To label proteins accessible from the cardiac vasculature in vivo, we perfused neonatal and adult hearts with a biotin-containing solution. The hearts were then homogenized and biotinylated proteins were enriched using streptavidin-conjugated beads for their identification with mass spectrometry. Bioinformatic analysis provided a list of proteins differentially expressed in neonatal and adult hearts from which we chose a candidate, lumican, for further analysis. We investigated the function of lumican in ECM organization and vessel formation both ex vivo and in vivo. Additionally, we identified MMP-14 as an essential mediator of lumican activity in the adult heart.

**Results:** In vivo proteomic analysis revealed higher levels of lumican and its receptor integrin beta 1 in vessels of the adult heart. We verified the expression of lumican around cardiac arteries by immunofluorescence and confirmed its higher expression by cardiac fibroblasts in adult compared to neonatal hearts. Overexpression of lumican by NIH 3T3 fibroblasts resulted in ECM remodelling and formation of perpendicular structures, which are known to contrast angiogenesis, resulting in reduced proliferation of primary cardiac endothelial cells. In addition, by Western blot we identified different glycosylation patterns of lumican in the adult and neonatal heart. Since the binding of lumican to the active site of MMP-14 is known to be modulated by its glycan chains, we compared MMP-14 activity in the adult and neonatal heart. Consistent with higher levels of lumican glycosylation in the adult heart, we registered lower levels of MMP-14 activity in this organ. The inhibitory activity of lumican on cardiac angiogenesis was confirmed in lumican knockout mice, which have more vessels in the heart compared to wild type animals.

**Conclusion:** We identified lumican as an ECM protein that exerts a potent anti-angiogenic effect in the adult heart. These results shed light on the importance of the vascular ECM in regulating cardiac angiogenesis and pave the way for novel regenerative therapies.